

SKA Data Challenge 3

Foreground removal update from SKACH team




SKACH

Michele Bianco
Tianyue Chen
Shreyam Krishna
Arpan Das

EPFL

Rohit Sharma

n|w

Sambit Kumar Giri



Philipp Denzel

zhaw

Hatem Ghorbel
Edouard Goffinet

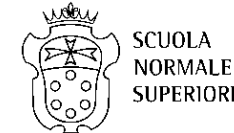
Hes.so

Massimo De Sanctis

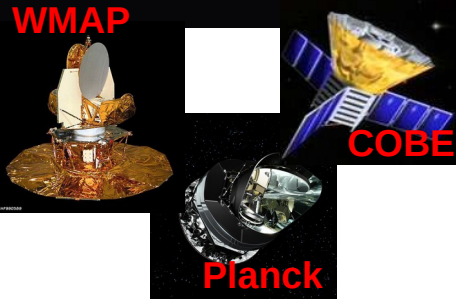
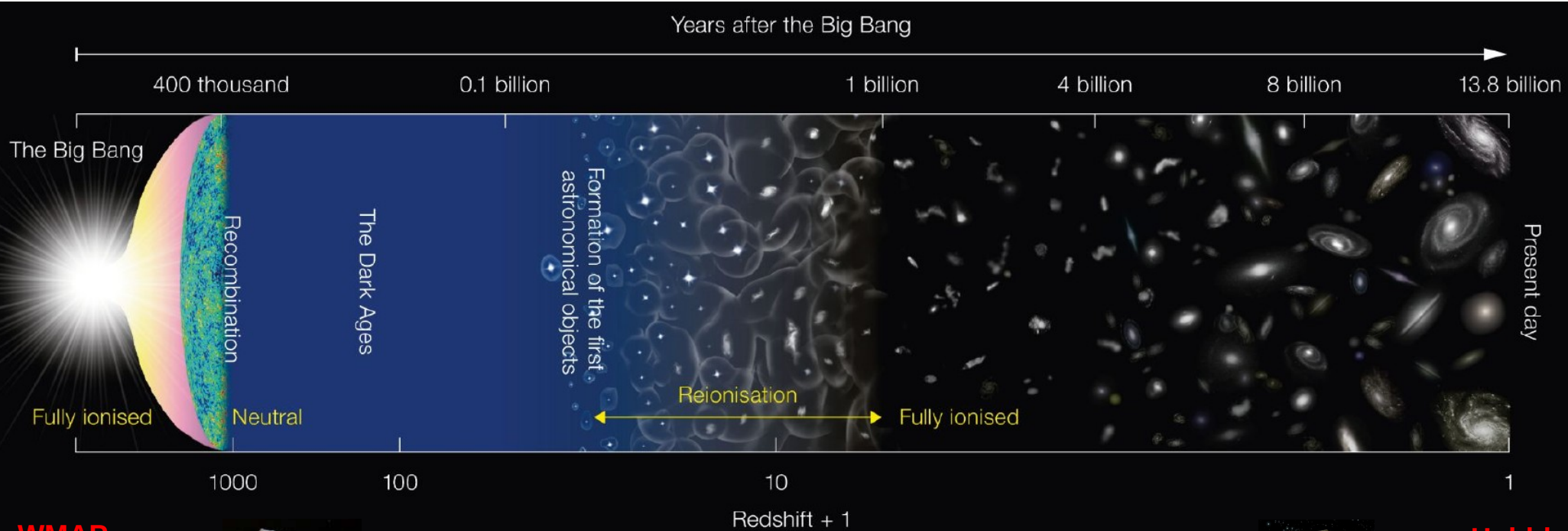
Viraj Nistane
Christopher Finlay



Andrei Mesinger
David Prelogović



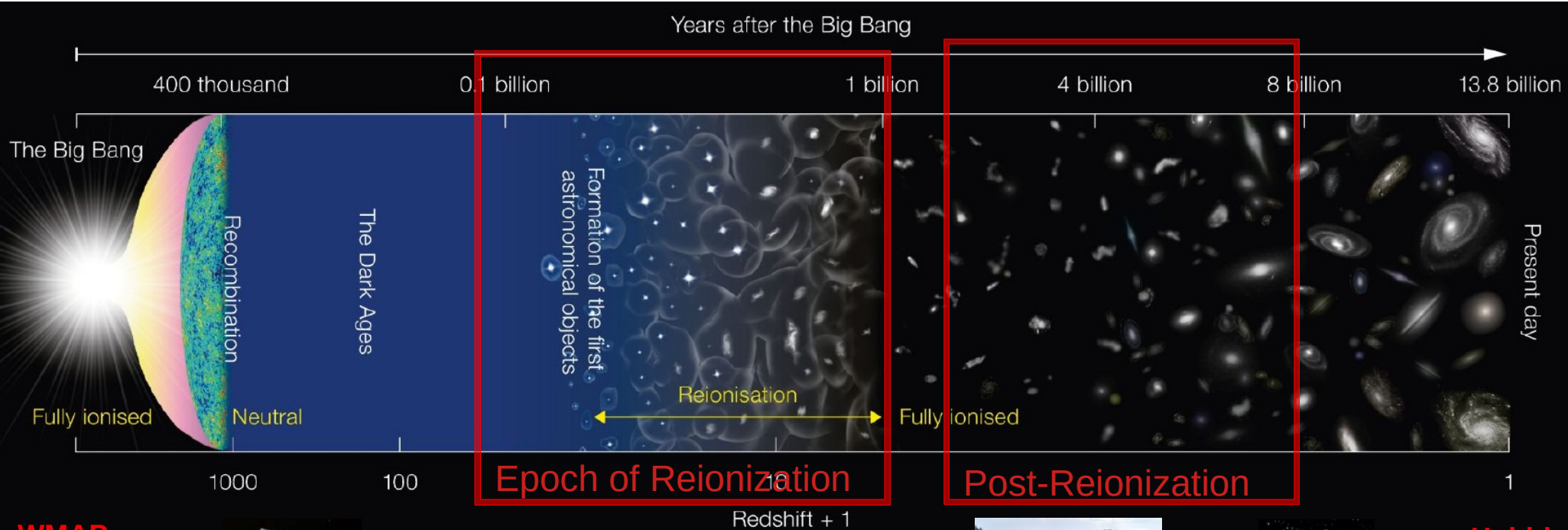
Cosmology with Radio Interferometric Experiments



Current cosmology is inferred by either larger scale or local cosmological constraints



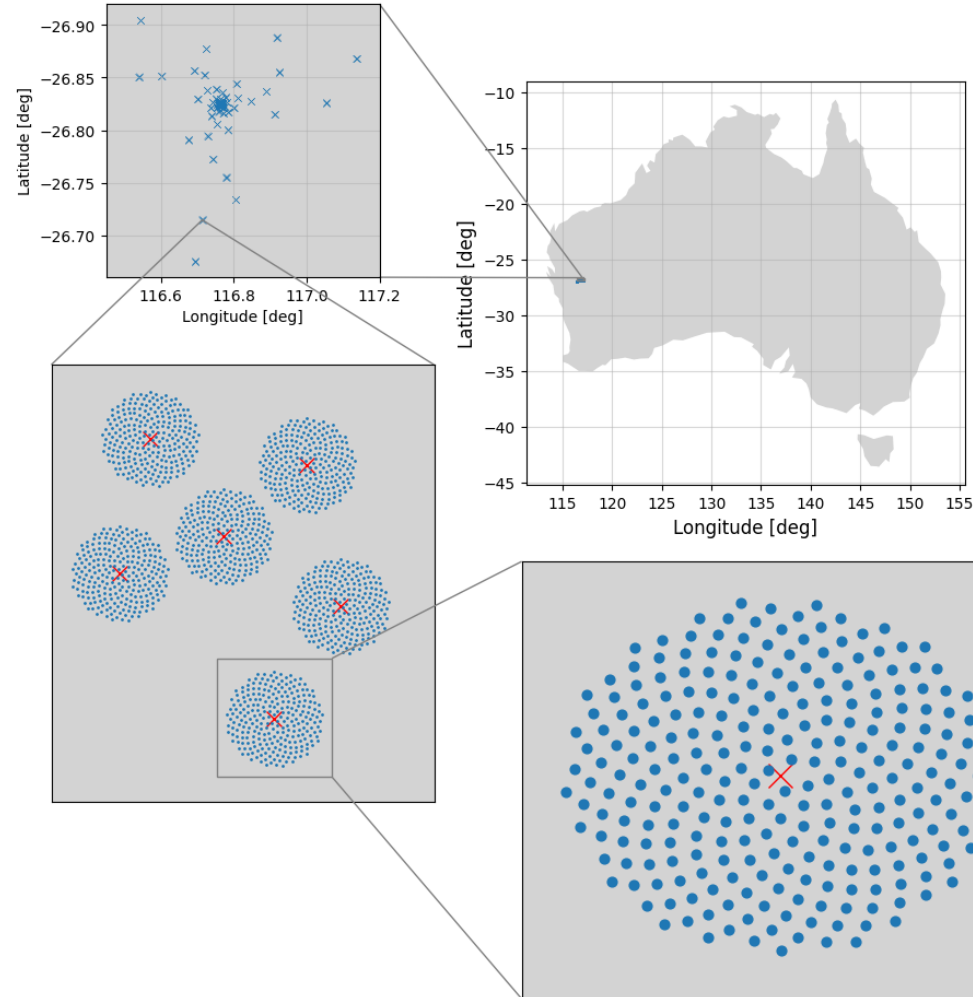
Cosmology with Radio Interferometric Experiments



Square Kilometre Array (SKA-Low)

Final layout of the SKA-Low stations and **start of the construction** on the 5th of December 2022.

- 512 stations, each with 128 antennas
- Maximum baseline ~65 km, station diameter 35 m
 - FoV = 10 deg with 16 arcsec resolution
- Frequency range between 50 to 350 MHz ($z = 27 - 5$)



Ongoing Radio Experiments

Emission at low frequency of the Galactic foreground sky and radio extra-galactic point sources.

Results from SKA pathfinder:

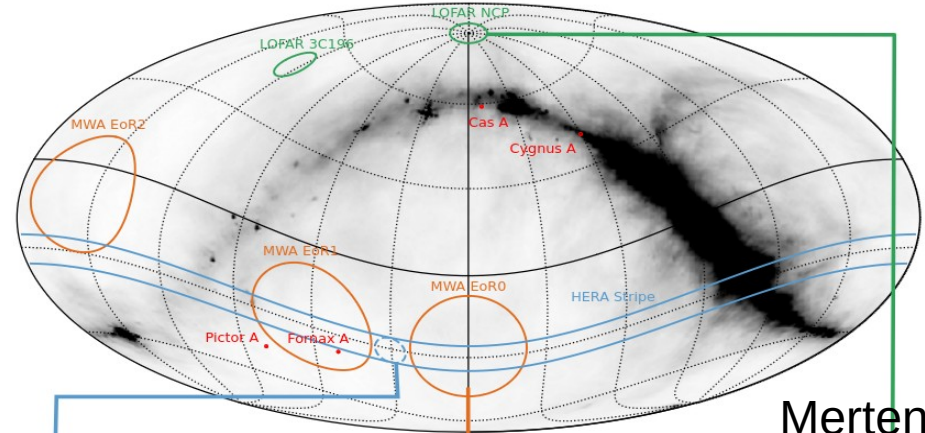
- HERA



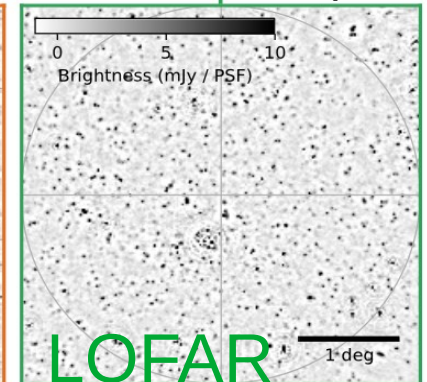
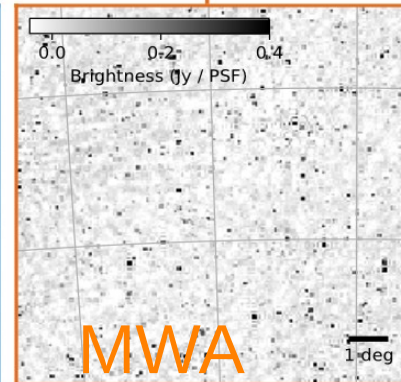
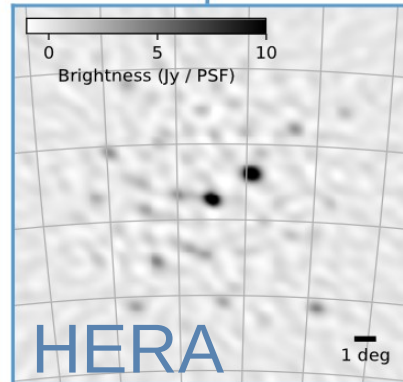
- MWA



- LOFAR



Mertens+ (2020)

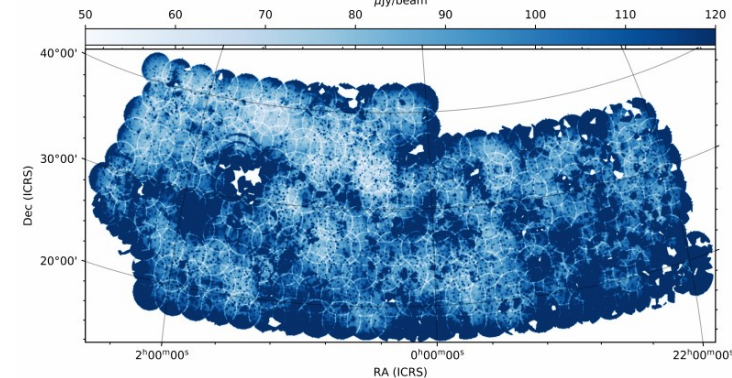
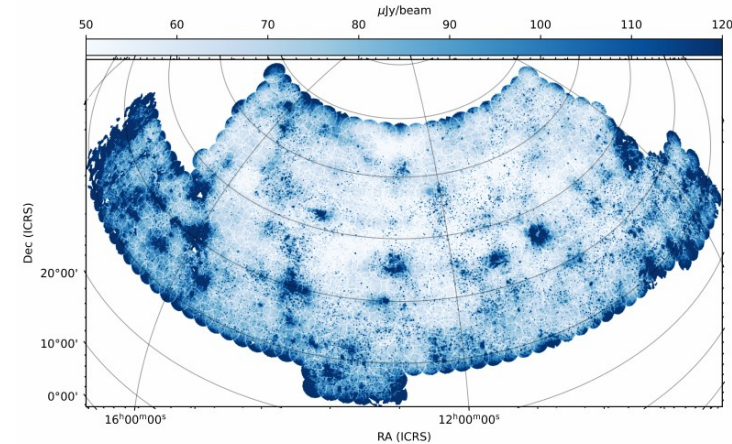
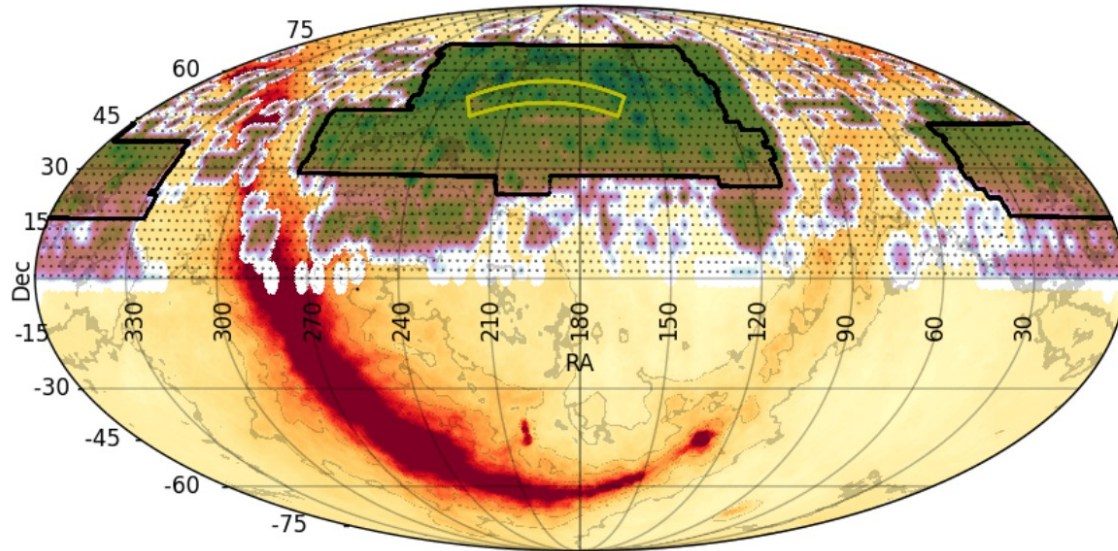


Ongoing Radio Experiments

LOFAR is covering 27% of North sky avoiding the Galactic plane.

Recent data release of the **LoTTS-DR2** observation:

- High Band Antenna: 120 – 168 MHz
- 3.4 hrs observation (7.6PB)

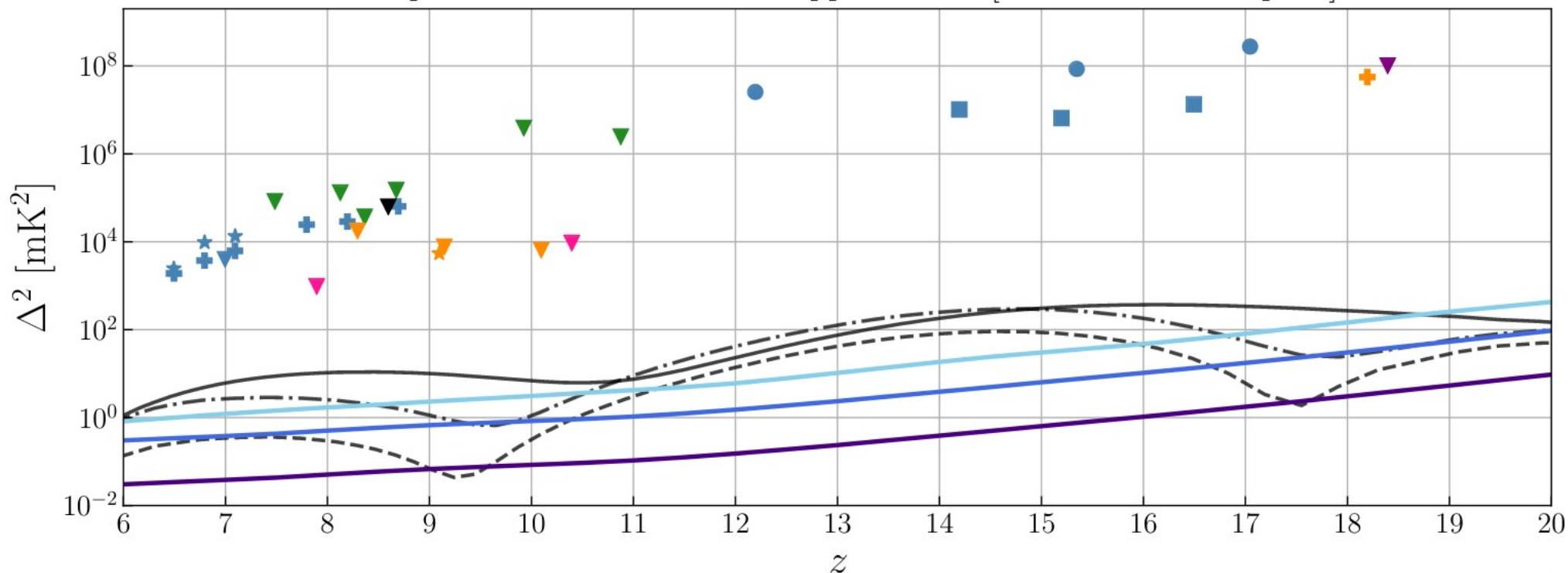


Shimwell+ (2022)



Constraints on the 21-cm Power Spectrum

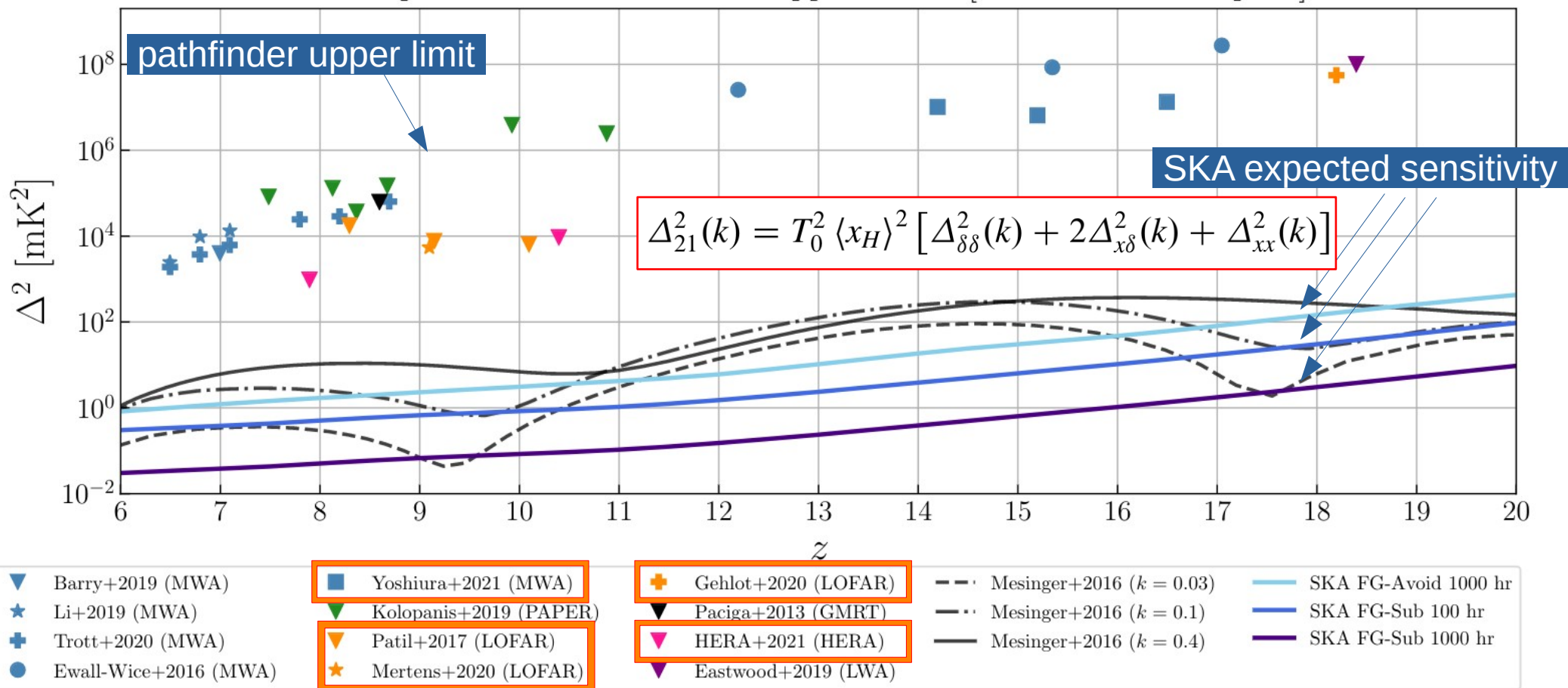
Power Spectrum 95% Confidence Upper Limits [$0.03 < k < 0.4 \text{ Mpc}^{-1}$]



Barry+ (2022)

Constraints on the 21-cm Power Spectrum

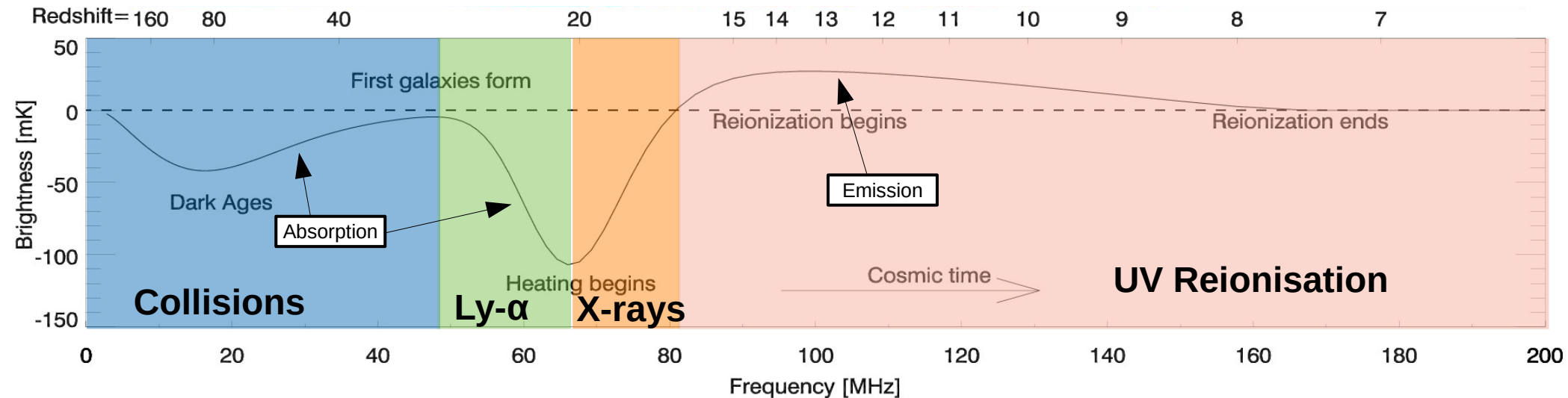
Power Spectrum 95% Confidence Upper Limits [$0.03 < k < 0.4 \text{ Mpc}^{-1}$]



The 21-cm Signal During EoR

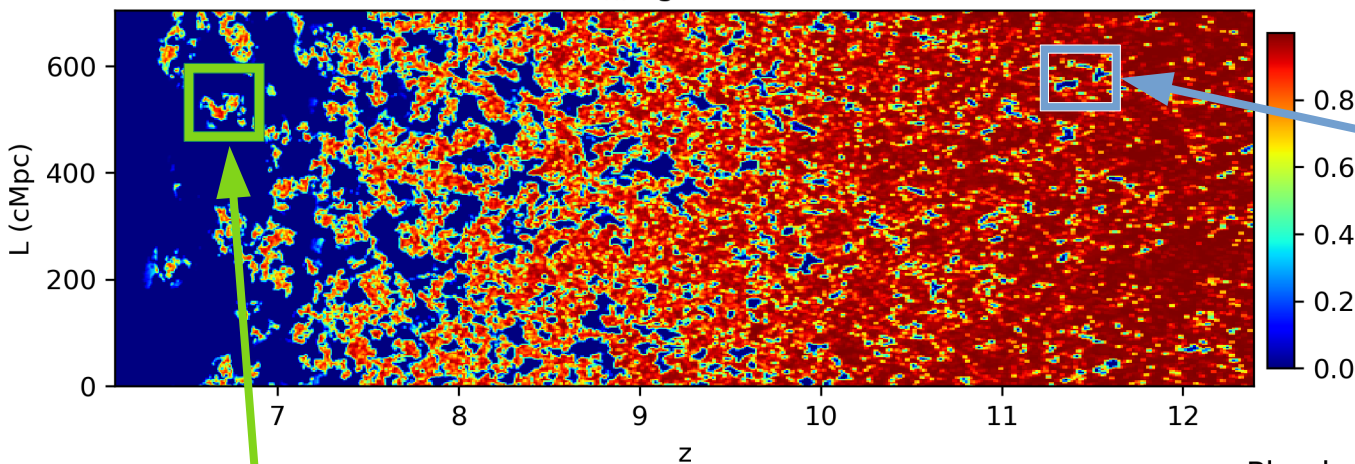
$$\delta T_b = 28\text{mK} (1 + \delta) x_{\text{HI}} \left(1 - \frac{T_{\text{CMB}}}{T_{\text{spin}}}\right) \left(\frac{\Omega_b h^2}{0.0223}\right) \sqrt{\left(\frac{1+z}{10}\right) \left(\frac{0.24}{\Omega_m}\right)} \left[\frac{H(z)/(1+z)}{dv_{\parallel}/dr_{\parallel}}\right]$$

↑ Gas density distribution
 ↑ Hydrogen Neutral fraction
 ↑ Spin temperature
 ↑ Cosmology
 ↑ L.o.S velocity



The 21-cm Signal During EoR

x_{HI} lightcone



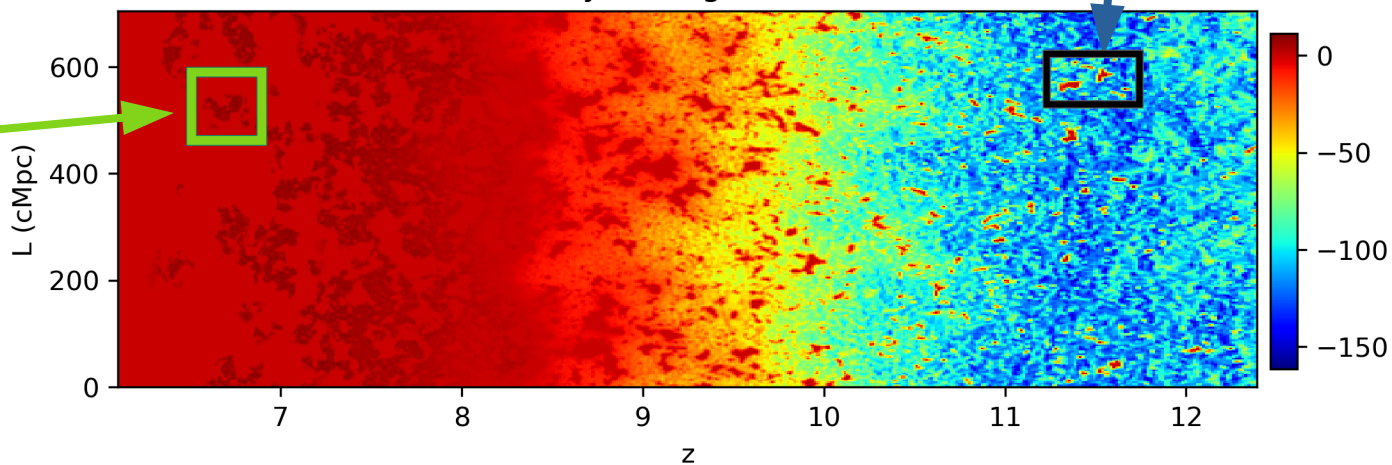
$$T_S \ll T_{\text{CMB}} \implies \delta T_b \ll 0 \text{ mK}$$

21-cm in emission
in cold IGM

21-cm emission
=
Neutral hydrogen

$$\delta T_b \propto x_{\text{HI}}(z)$$

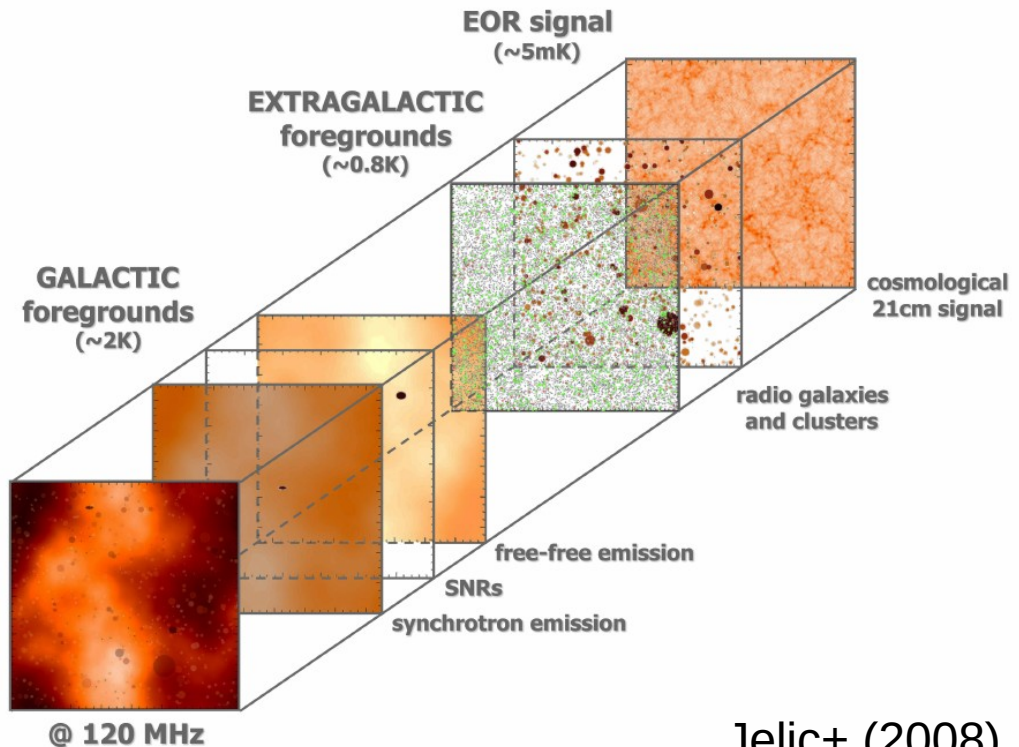
Physical lightcone



Tomographic Imaging of the 21-cm signal

SKA1-Low tomographic images of redshifted 21-cm signal challenges:

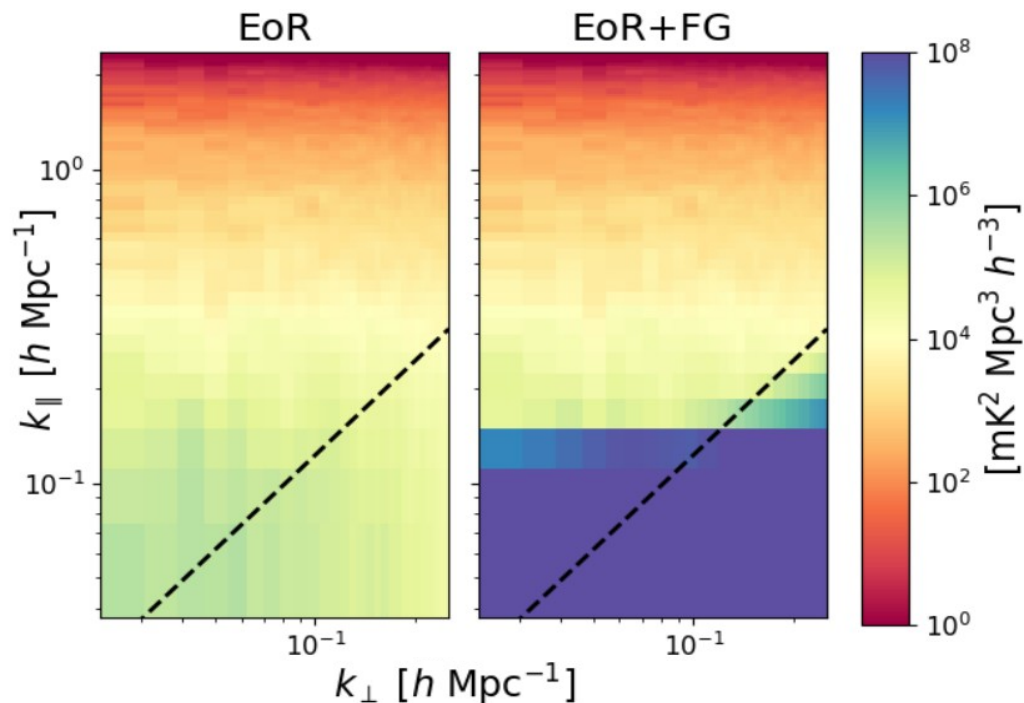
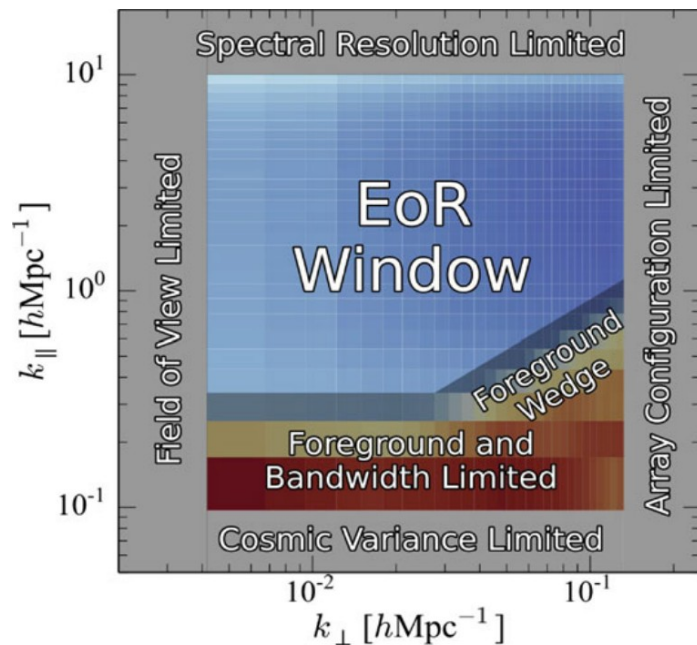
- Instrumental noise (signal ~ 5 K)
- Foreground emission (signal $\sim 1 - 1000$ K)
- Antennas gain errors
- Ionospheric refraction effects
- Radio frequency interference
- And more ...



Contamination from Galactic & extra-galactic Foregrounds

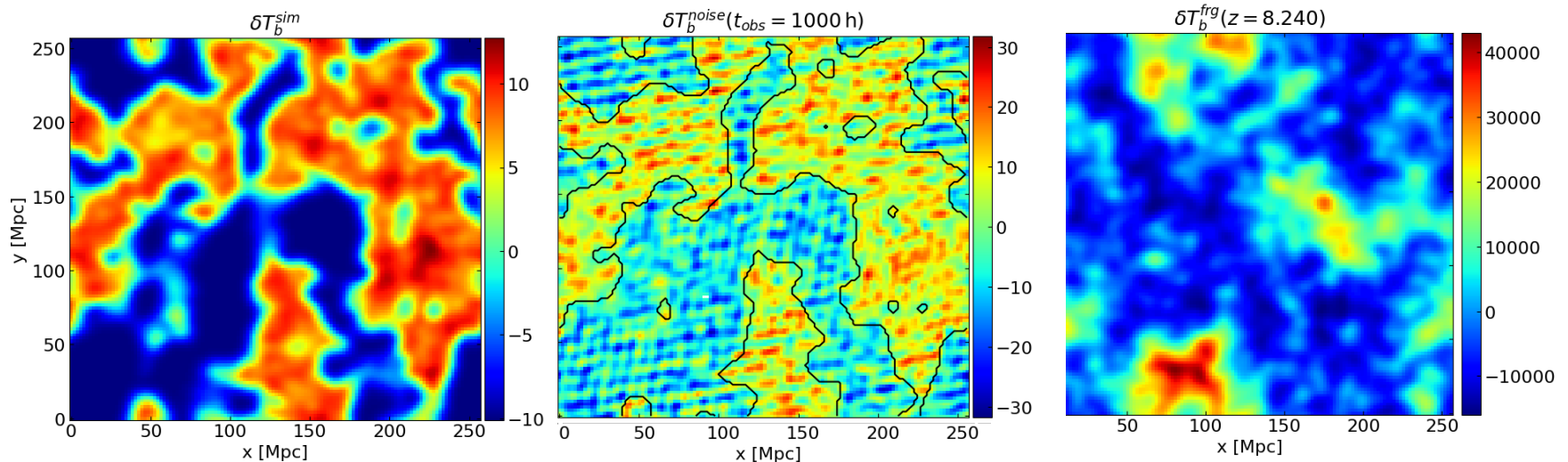
Most **foregrounds** have **frequency smooth spectra** compared to the 21-cm signal.

From 2D power spectra, remove $k_{\perp} - k_{\parallel}$ modes that are contaminated by the foregrounds as a **avoidance technique** or model them for **subtraction**.



Mock Data for 21-cm Observation

Currently we can create EoR mock observation with a combination of numerical models for 21-cm, systematic noise and Galactic foreground.

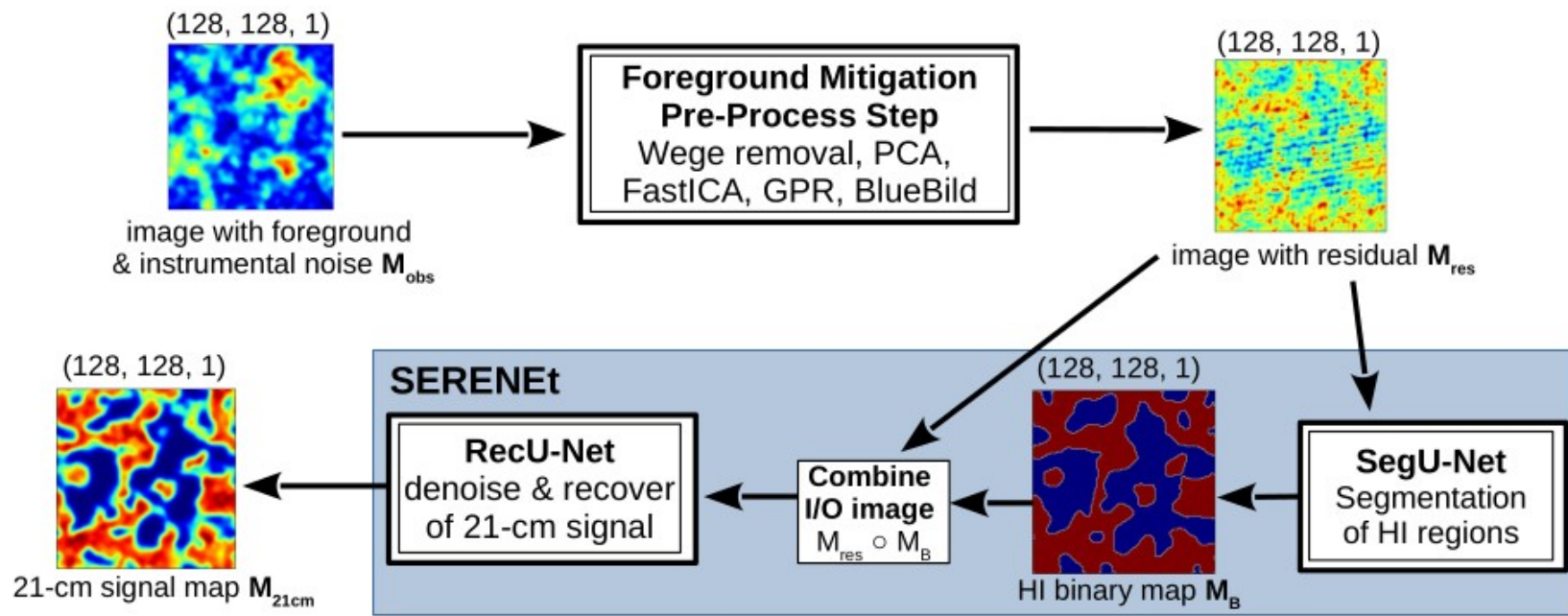


Goal:
pipelines to recover differential brightness and the distribution of neutral hydrogen from mock observations.

SERENet

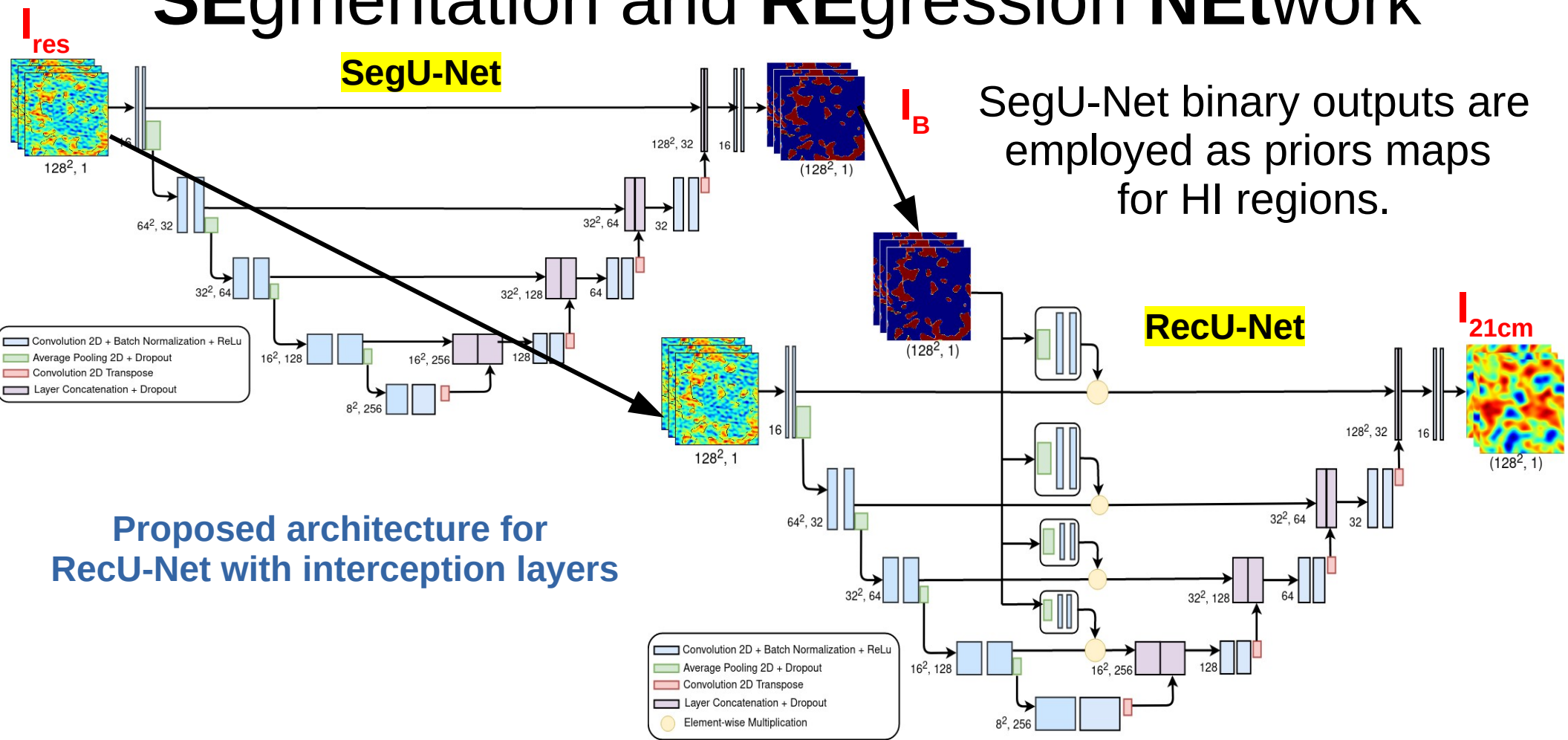
SEgmentation and REgression NEtwork

Combine the predicted binary maps of **SegU-Net** as additional input of **RecU-Net** training step in order to include prior in the network training.



SERENet

SEgmentation and REgression NETWORK

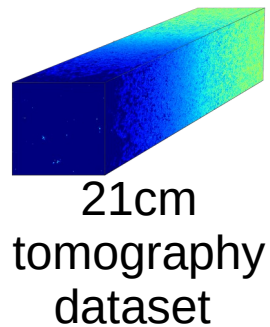


SegU-Net: Segmentation with U-Net

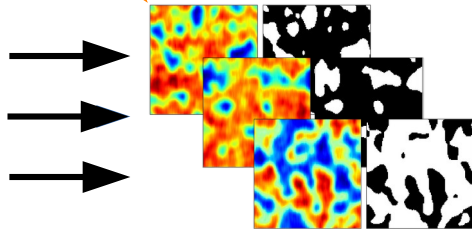
(Bianco+ 2021, 2023)

- U-Net:
Network with interconnected
encoder/decoder layers

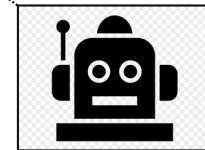
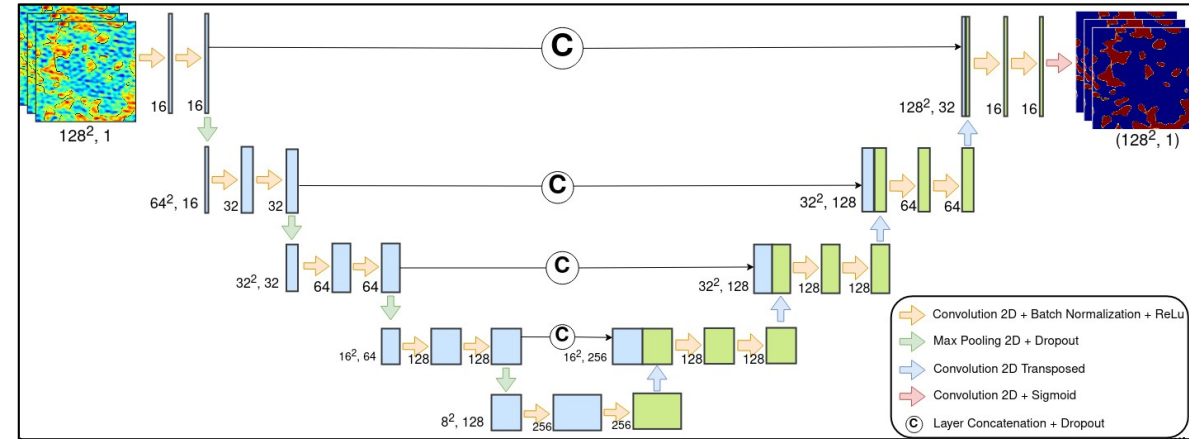
add PCA pre-process
step that decreases
image dynamic range



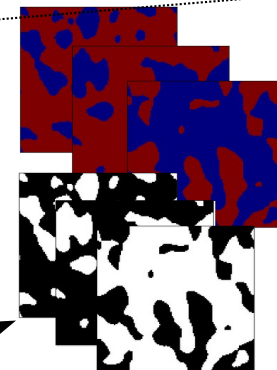
21cm
tomography
dataset



21cm signal = image
 x_{HI} field = mask



SegU-Net
(2.5M trainable params.)



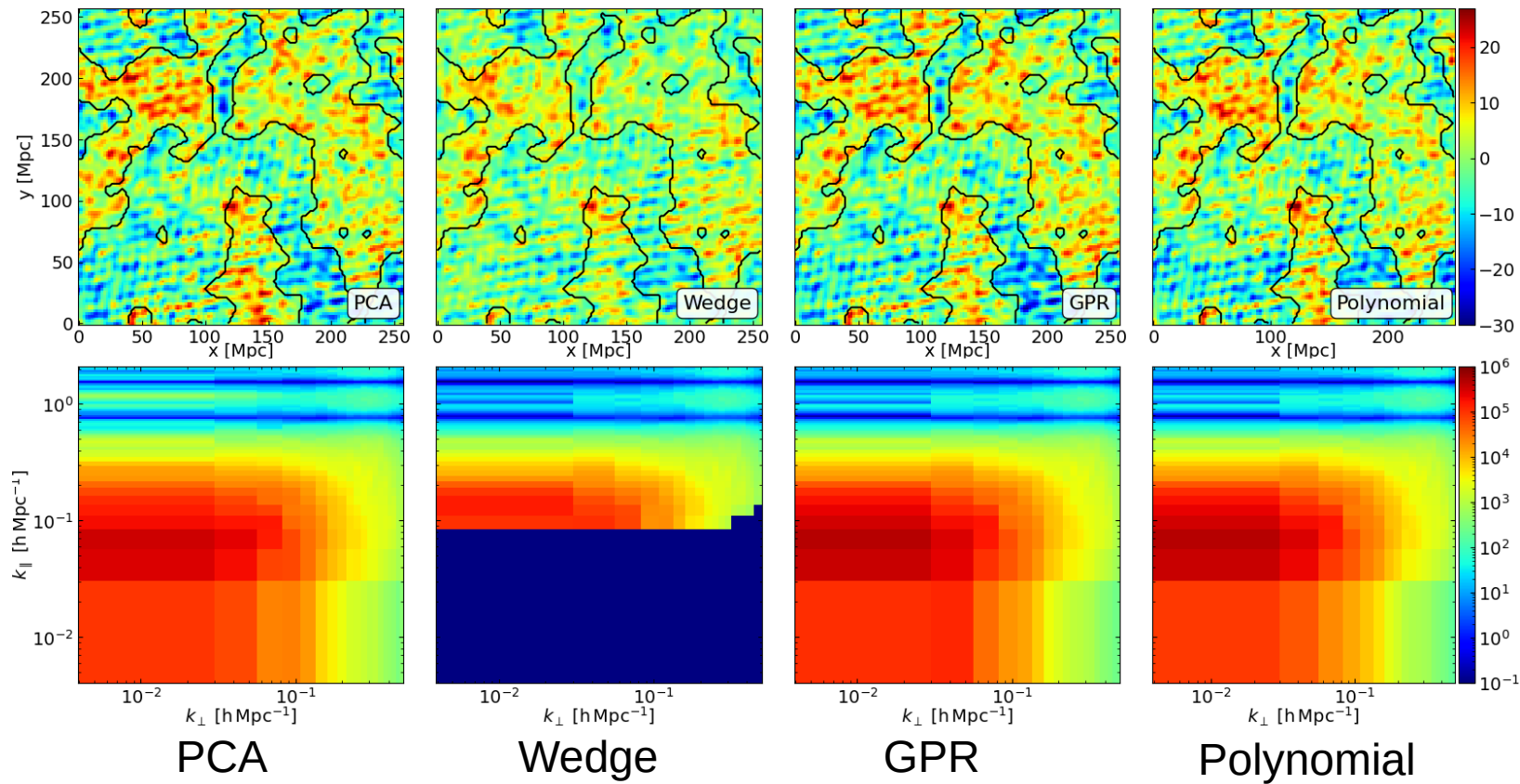
Compare
Prediction/True mask

$$\mathcal{L}(y, \hat{y})$$

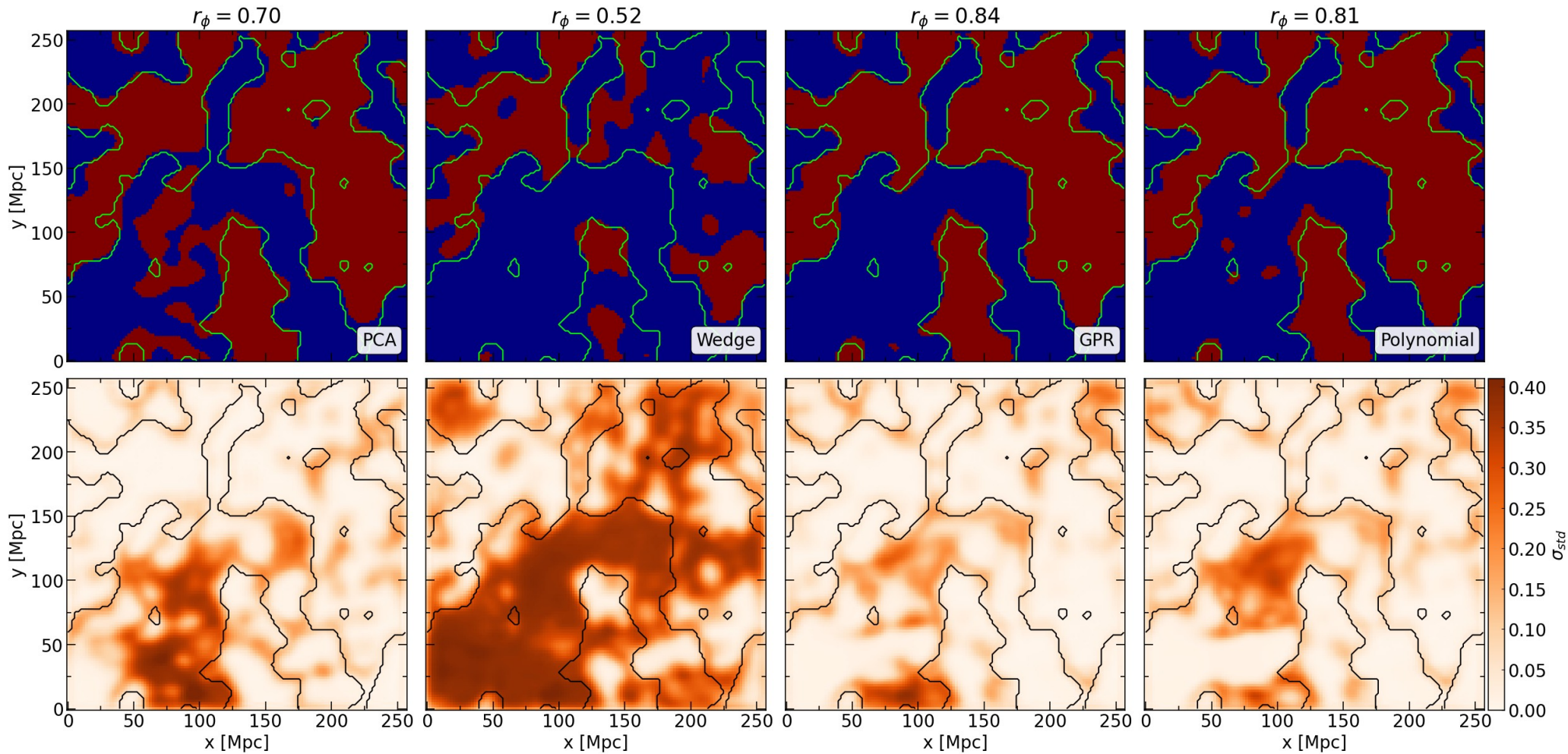
Calculate
Loss

Pre-process: Foreground Mitigation & Avoidance

We employ 3 mitigation and 1 avoidance techniques, Bianco+ 2023

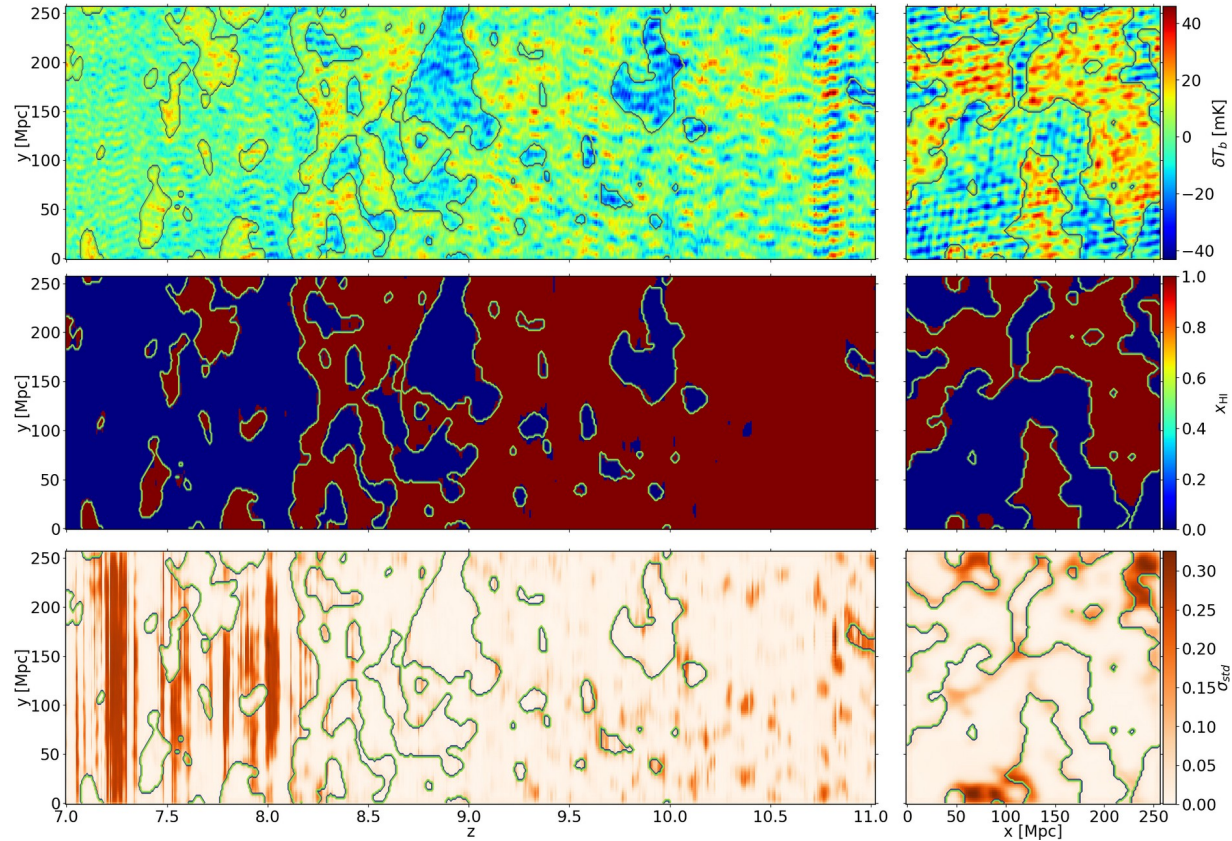
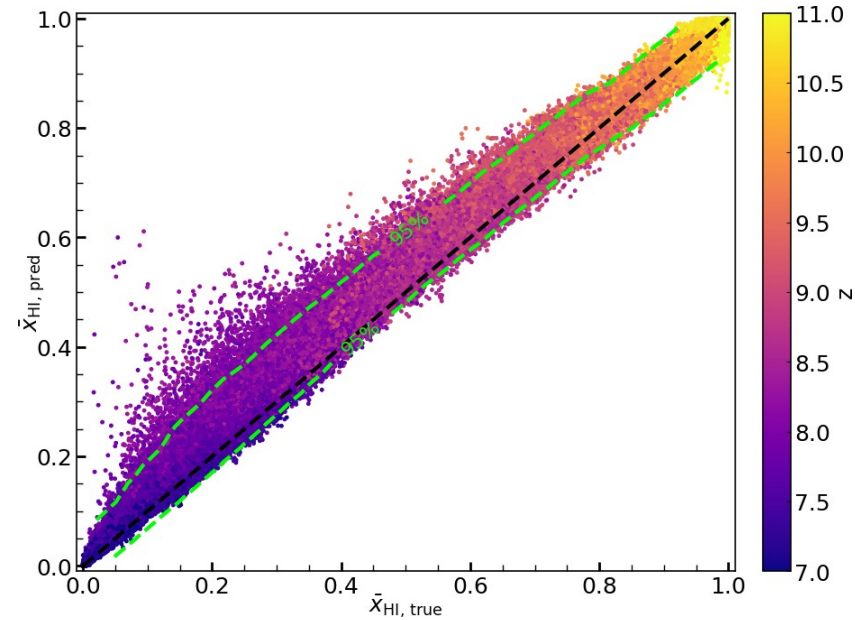


SDC3: General Announcement



SegU-Net: Tomographic Data & Reionization History

z_c	pre-process	\bar{x}_{HI}
8.24	Ground Truth	0.45
	all z PCA	0.48 ± 0.07
	PCA	0.49 ± 0.11



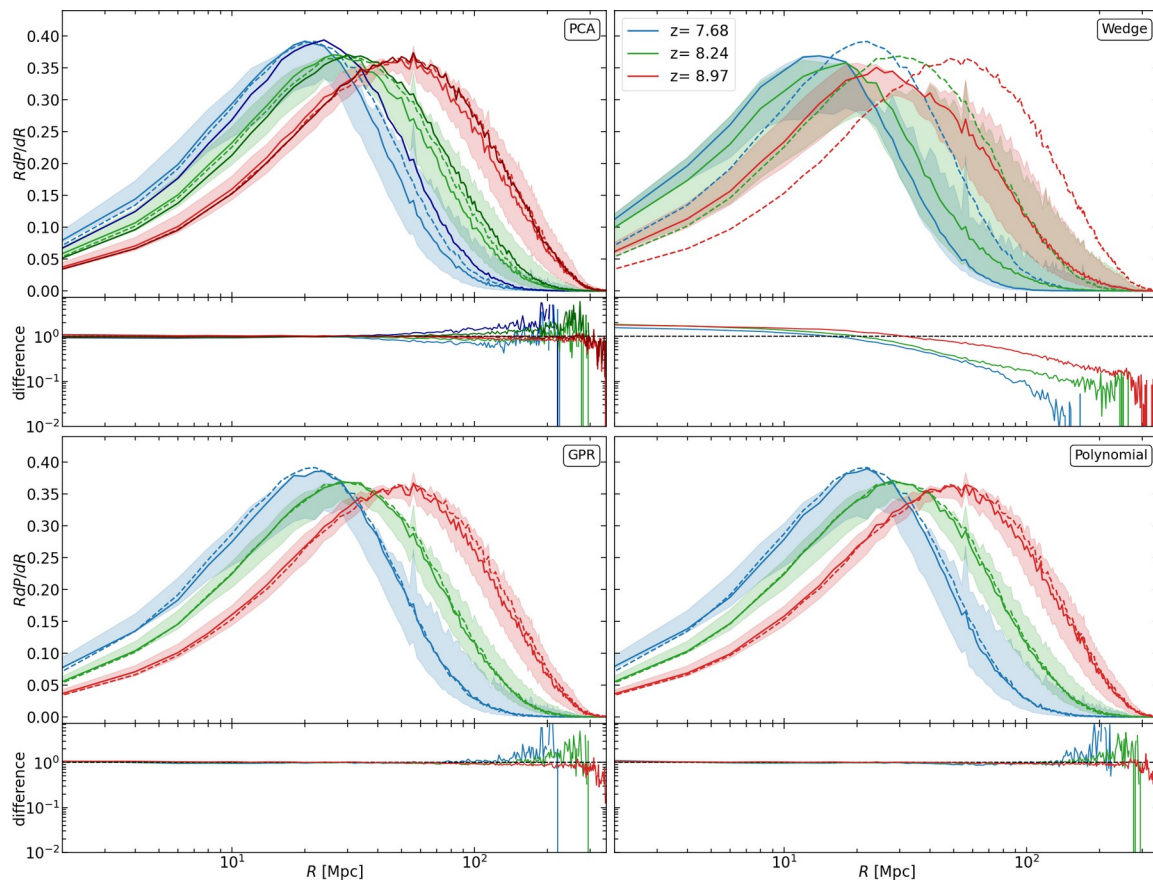
SegU-Net: HI size distribution

The Island (HI regions) size distribution is an powerful probe of the reionization process. (21-cm non-Gaussianity)

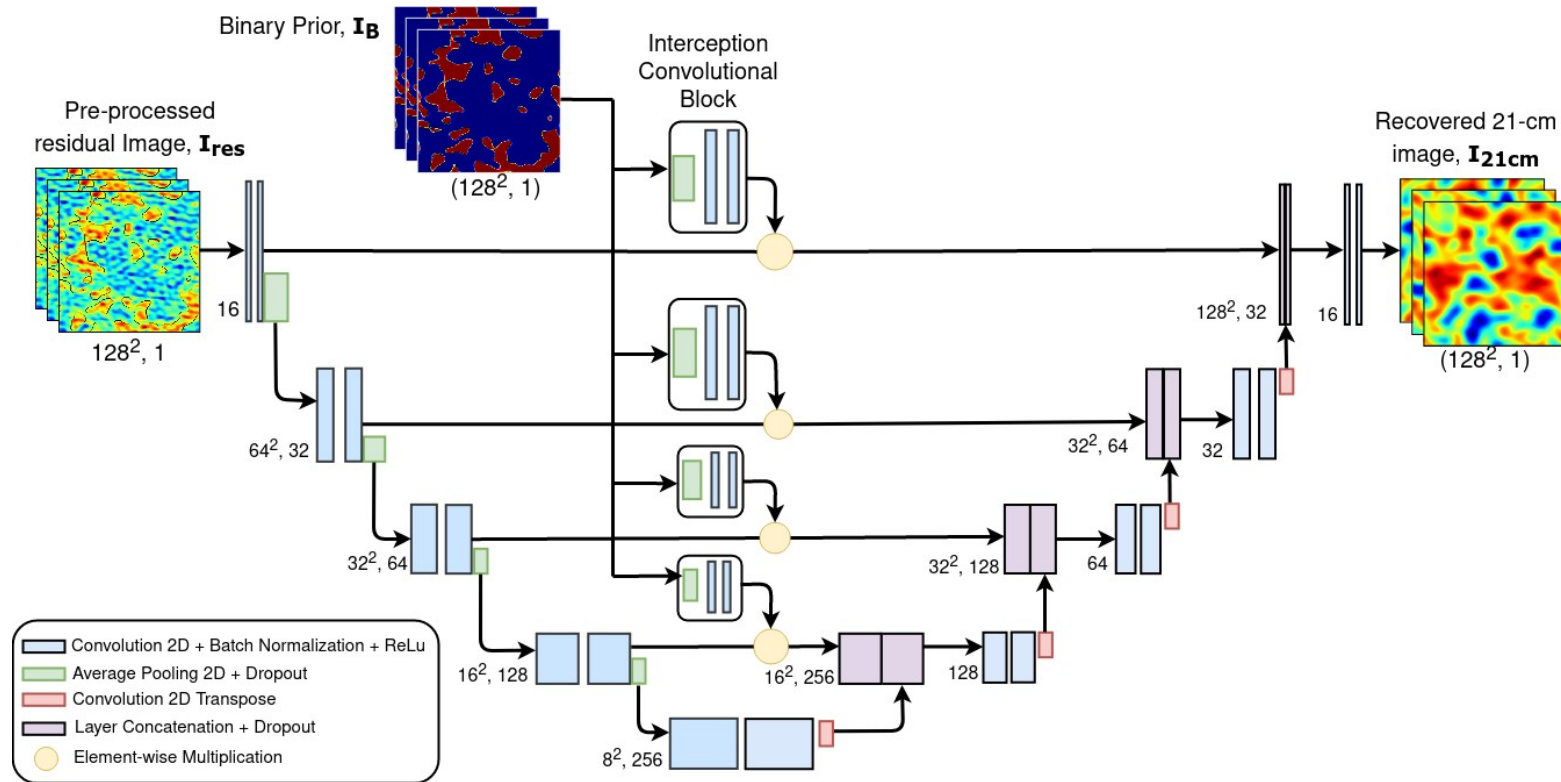
$$\bar{R}_C(z) = \int_{R_{\min}}^{\infty} R \frac{dP}{dR}(z) dR$$

SegU-Net results:

z_c	pre-process	\bar{R}_C [cMpc]
8.24	Ground Truth	29.54
	all z PCA	31.37 ^{+3.09} _{-3.93}
	PCA	27.65 ^{+9.13} _{-6.12}
	Wedge	15.20 ^{+24.13} _{-6.18}
	GPR	29.14 ^{+5.26} _{-4.89}
	Polynomial	29.21 ^{+5.83} _{-5.21}



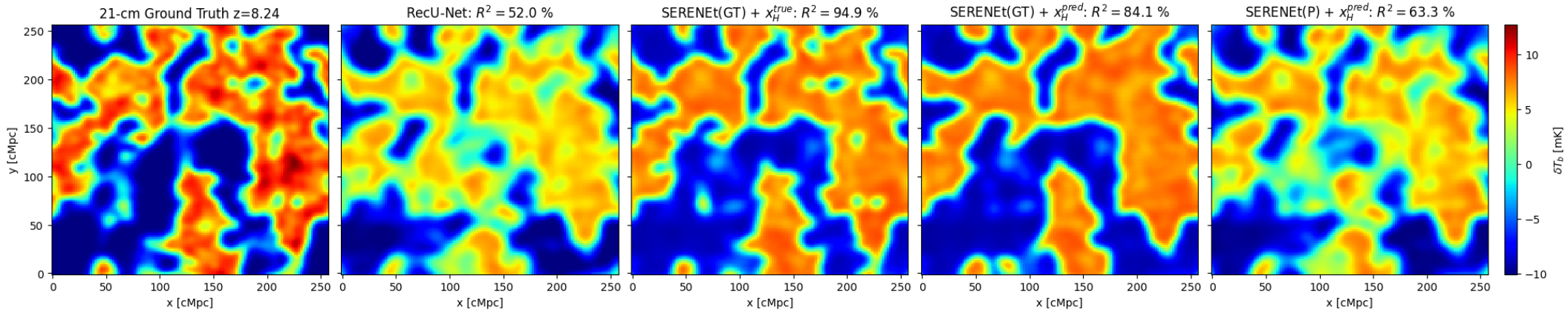
RecU-Net: Recover 21-cm with U-Net (Bianco+ in prep.)



U-Net architecture with intercepting convolution block to process the binary prior map from SegU-Net

SERENet: Recover of 21-cm Signal

Recovered 21-cm signal for EoR for image at $z = 8.25$ ($x_{\text{HI}} \sim 0.5$)



Best performing setup consider:

- Train SERENet with the prior binary ground truth: **SERENet(GT)**
- Real application requires the predicted binary map from SegU-Net for the prediction: **SERENet(GT) + $x_{\text{HI}}^{\text{pred}}$**

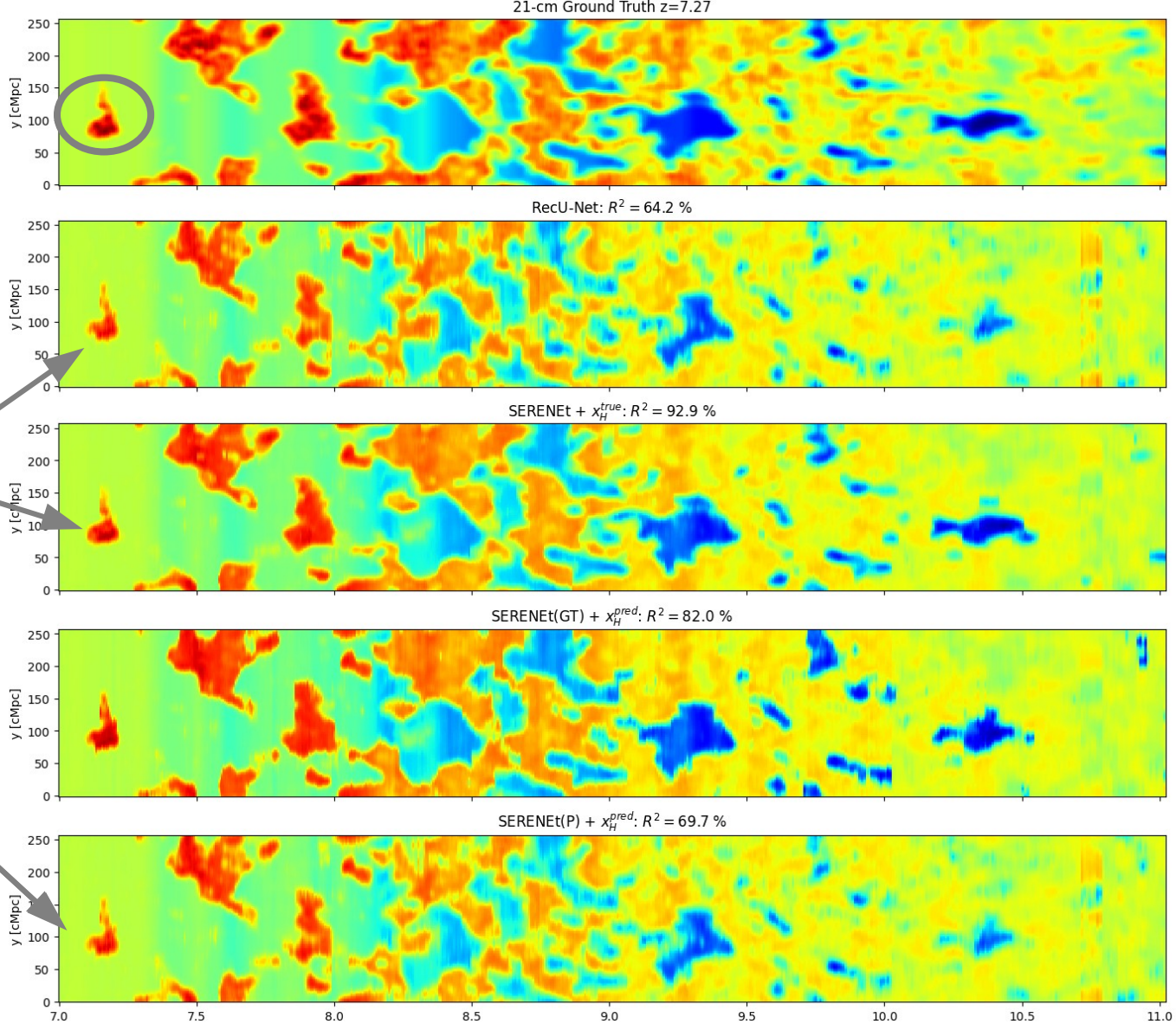
SERENet

Limitation at lower redshift and decrease in accuracy for:

SERENet(GT) + x_H^{pred}

When compared to

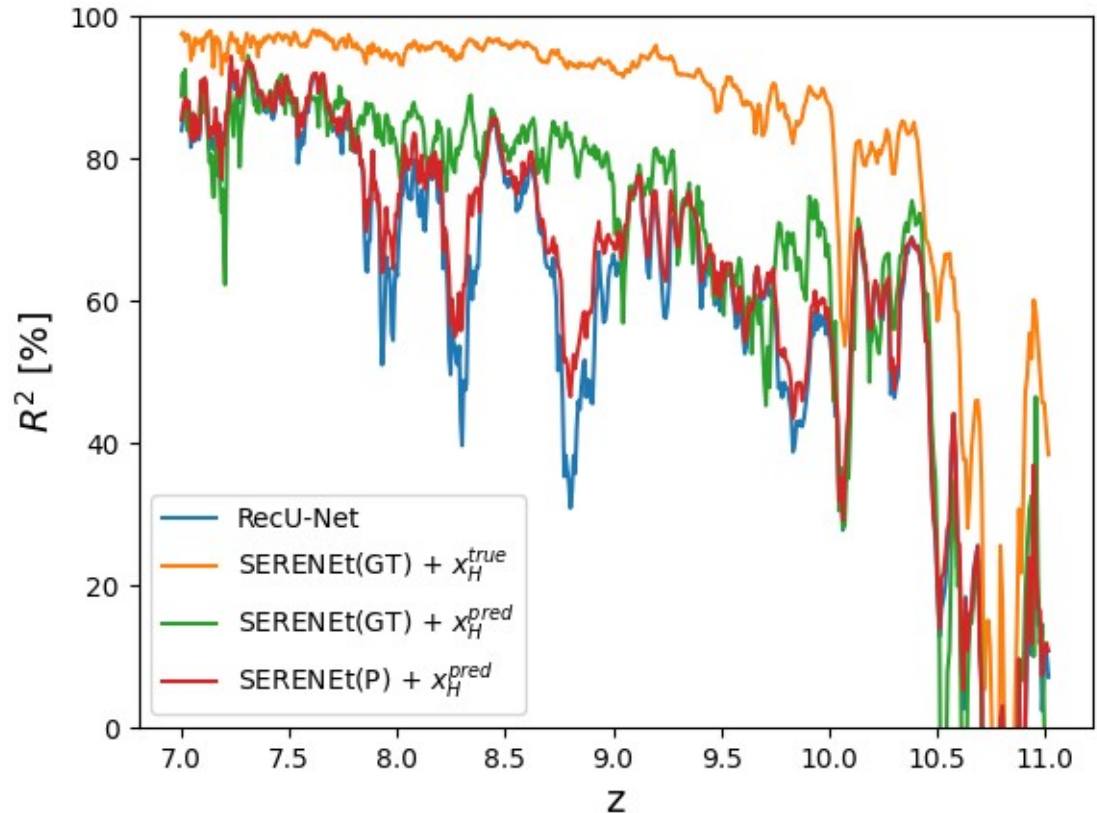
**RecU-Net or
SERENet(P) + x_H^{pred}**



SERENet: Recover of 21-cm Signal

Coefficient of determination (R^2 score) redshift evolution as a temporary
Figure of Merit metric (FoM):

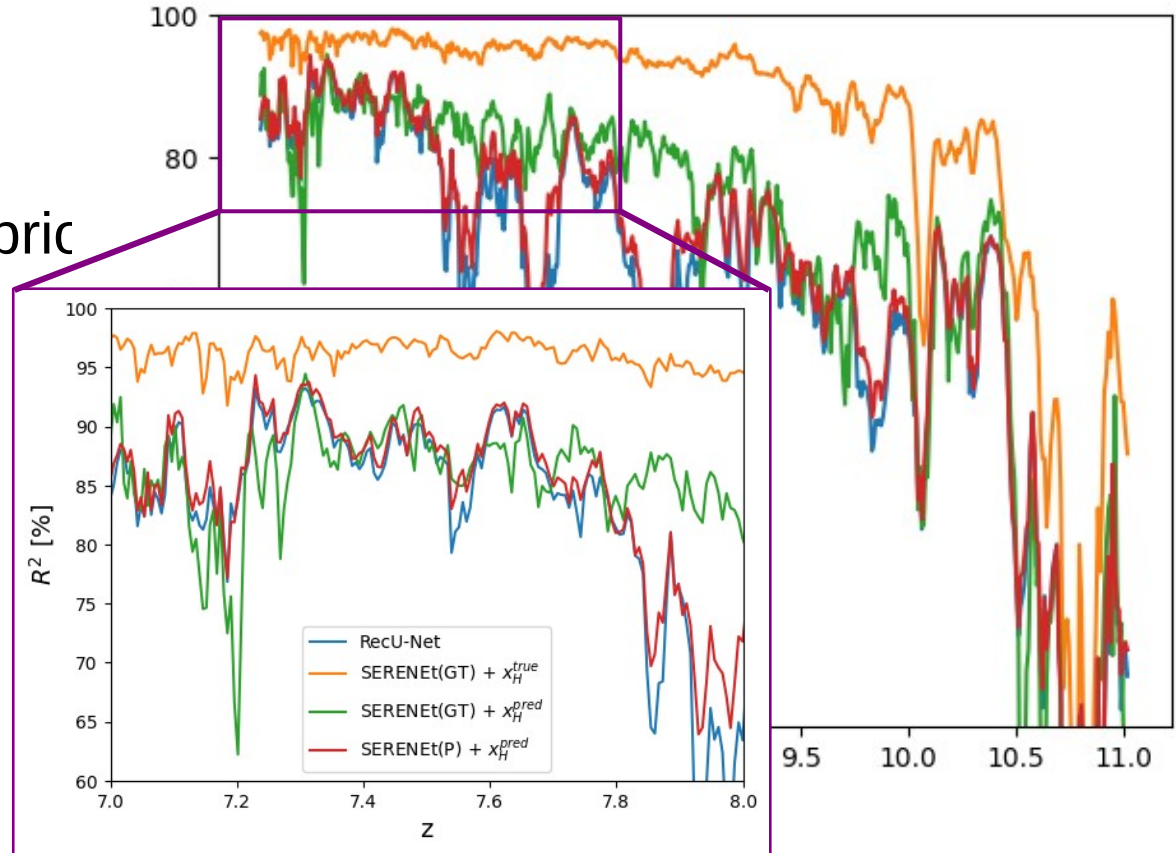
- **SERENet(GT) + x_H^{true}**
upper limit based on best price
binary map (ground truth)
- **SERENet(GT) + x_H^{pred}**
next best results when
compared to **RecU-Net** or
SERENet(P) + x_H^{pred}



SERENet: Recover of 21-cm Signal

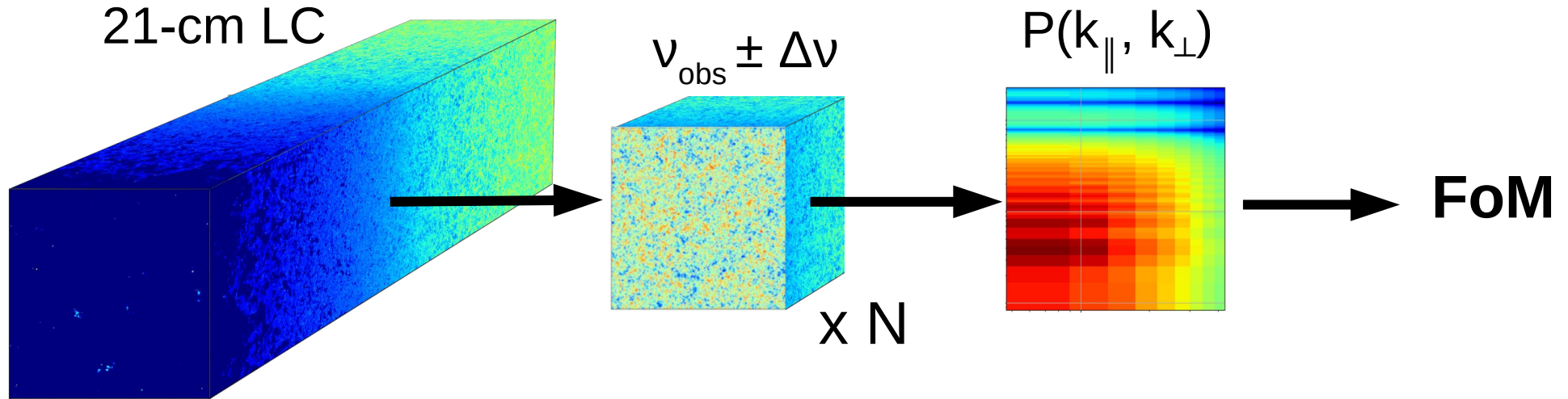
Coefficient of determination (R^2 score) redshift evolution as a temporary
Figure of Merit metric (FoM):

- **SERENet(GT) + x_H^{true}**
upper limit based on best price
binary map (ground truth)
- **SERENet(GT) + x_H^{pred}**
next best results when
compared to **RecU-Net** or
SERENet(P) + x_H^{pred}



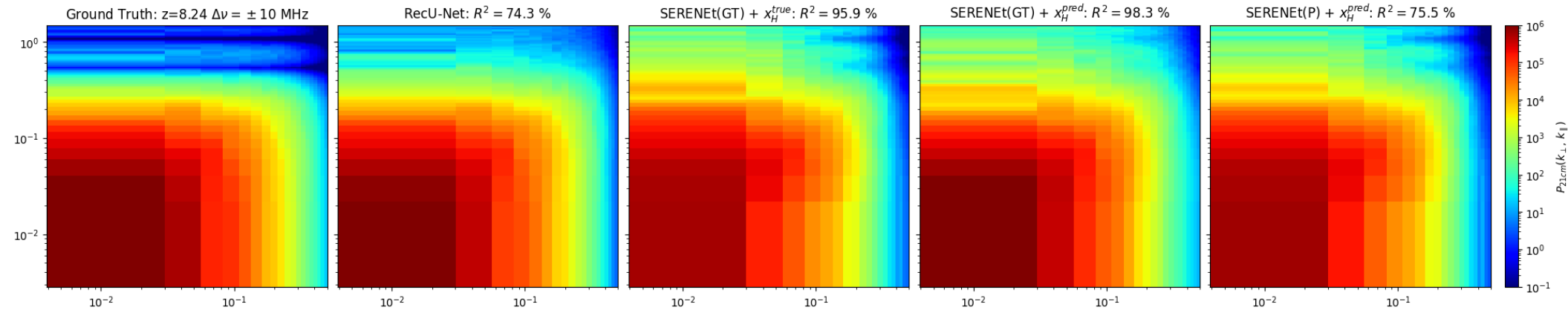
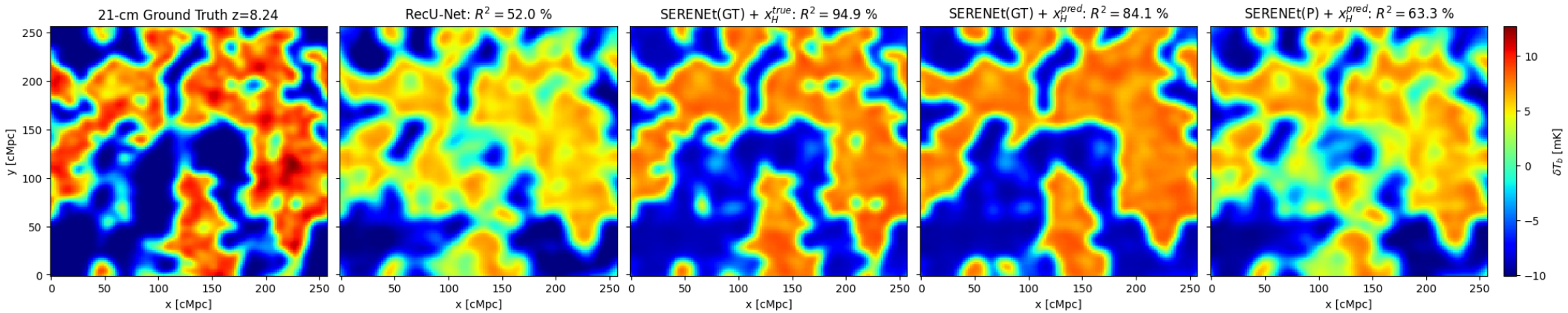
SDC3 Scoring System

The Figure of Merit (FoM) based on “*metric distance*” between the true and recovered spectra for **N sub-volumes** at a central frequency ν_{obs} and width $\Delta\nu$



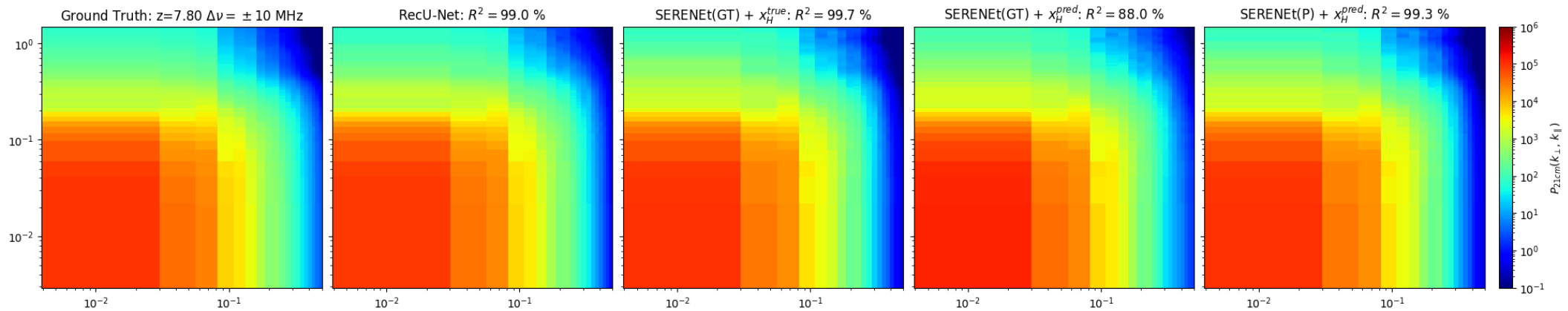
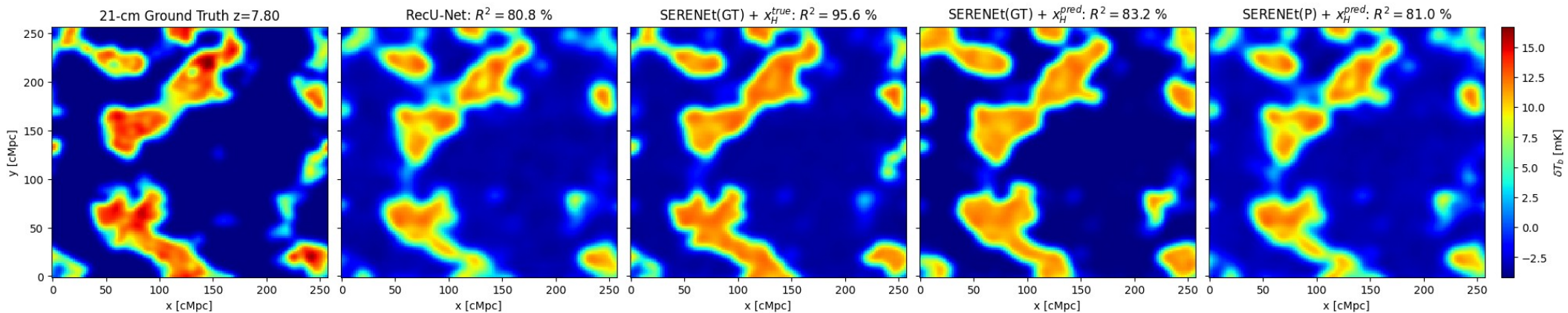
SERENEt: Recover of 21-cm Signal

Recovered 21-cm signal for EoR for lightcone subvolume centered at redshift $z = 8.25$ ($x_{\text{HI}} \sim 0.5$) and $\Delta\nu \pm 10$ MHz



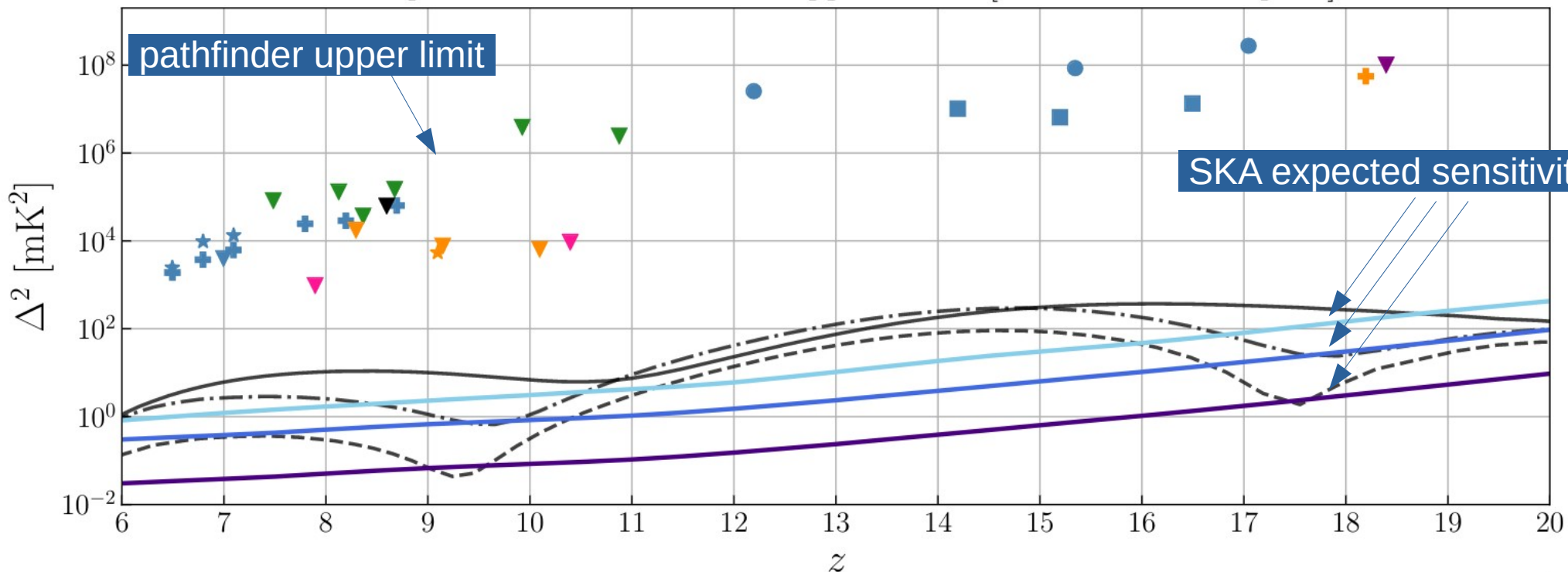
SERENet: Recover of 21-cm Signal

Recovered 21-cm signal for EoR for lightcone subvolume centered at redshift $z = 7.8$ ($x_{\text{HI}} \sim 0.3$) and $\Delta\nu \pm 10$ MHz



SERENet: Comparison with Current Data

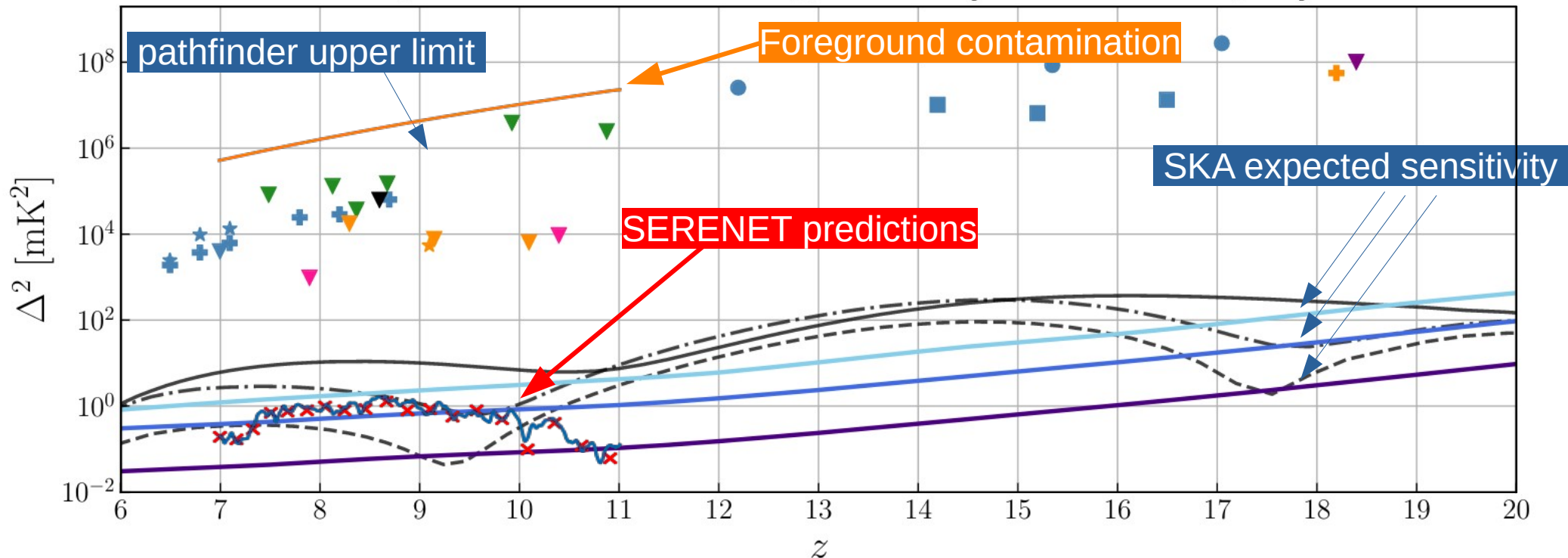
Power Spectrum 95% Confidence Upper Limits [$0.03 < k < 0.4 \text{ Mpc}^{-1}$]



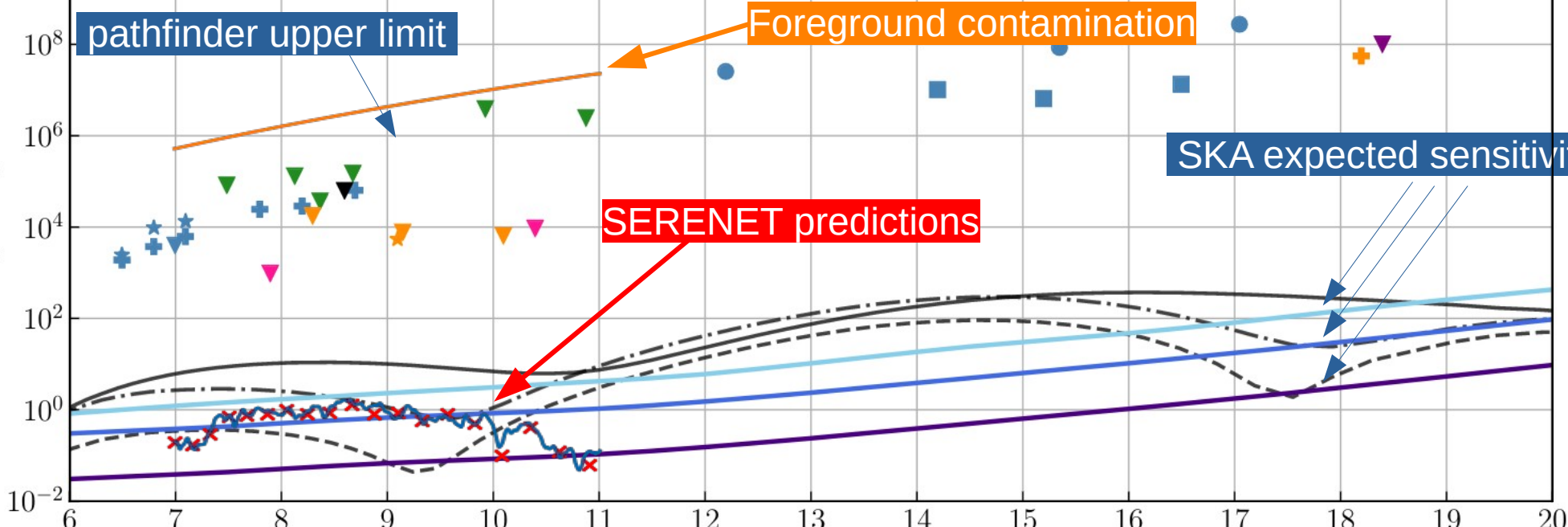
Barry+ (2022)

SERENet: Comparison with Current Data

Power Spectrum 95% Confidence Upper Limits [$0.03 < k < 0.4 \text{ Mpc}^{-1}$]



$\Delta^2 \text{ [mK}^2\text{]}$



z

- | | | | | |
|-------------------------|--------------------------|-----------------------|------------------------------------|------------------------|
| ▼ Barry+2019 (MWA) | ■ Yoshiura+2021 (MWA) | ✦ Gehlot+2020 (LOFAR) | - - · Mesinger+2016 ($k = 0.03$) | — SKA FG-Avoid 1000 hr |
| ★ Li+2019 (MWA) | ▼ Kolopanis+2019 (PAPER) | ▼ Paciga+2013 (GMRT) | - · · Mesinger+2016 ($k = 0.1$) | — SKA FG-Sub 100 hr |
| ⊕ Trott+2020 (MWA) | ▼ Patil+2017 (LOFAR) | ▼ HERA+2021 (HERA) | — Mesinger+2016 ($k = 0.4$) | — SKA FG-Sub 1000 hr |
| ● Ewall-Wice+2016 (MWA) | ★ Mertens+2020 (LOFAR) | ▼ Eastwood+2019 (LWA) | | |

Thanks

Support Slides

Mesinger+ (2016)

$\delta(\mathbf{r}, z)$: Dark matter density fluctuations depends on structure formation

$x_{\text{HI}}(z)$: Volume neutral fraction depends on SFH in the early Universe

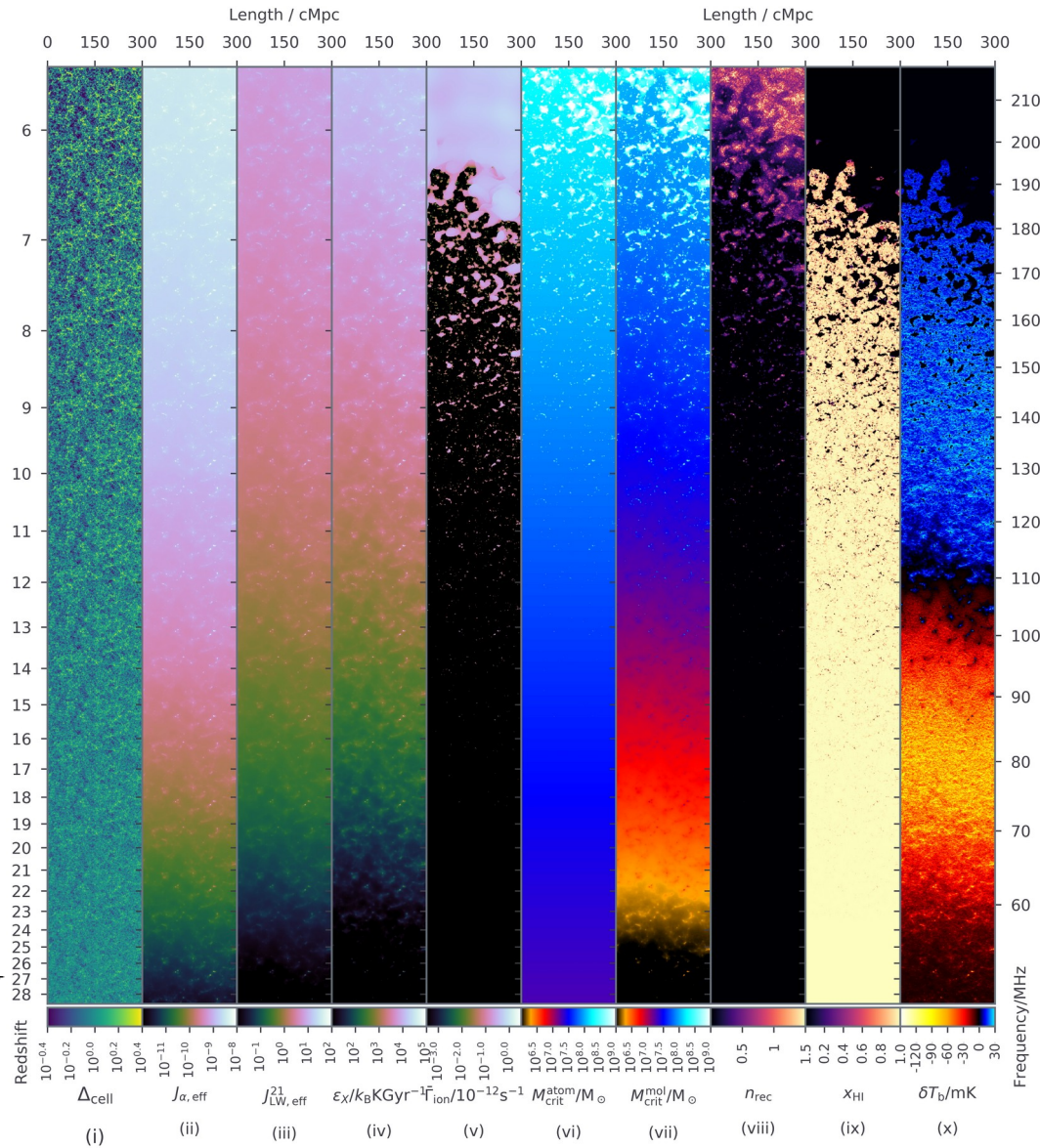
$$T_S^{-1} = \frac{T_{\text{CMB}}^{-1} + x_\alpha T_\alpha^{-1} + x_c T_K^{-1}}{1 + x_\alpha + x_c}$$

$x_\alpha \propto J_\alpha(z)$

Wouthuysen-Field effect (Ly α pumping)

$$x_c = x_c^{\text{HH}} + x_c^{\text{eH}} + x_c^{\text{pH}}$$

Collision coupling



Mesinger+ (2016)

$\delta(\mathbf{r}, z)$: Dark matter density fluctuations depends on structure formation

$x_{\text{HI}}(z)$: Volume neutral fraction depends on SFH in the early Universe

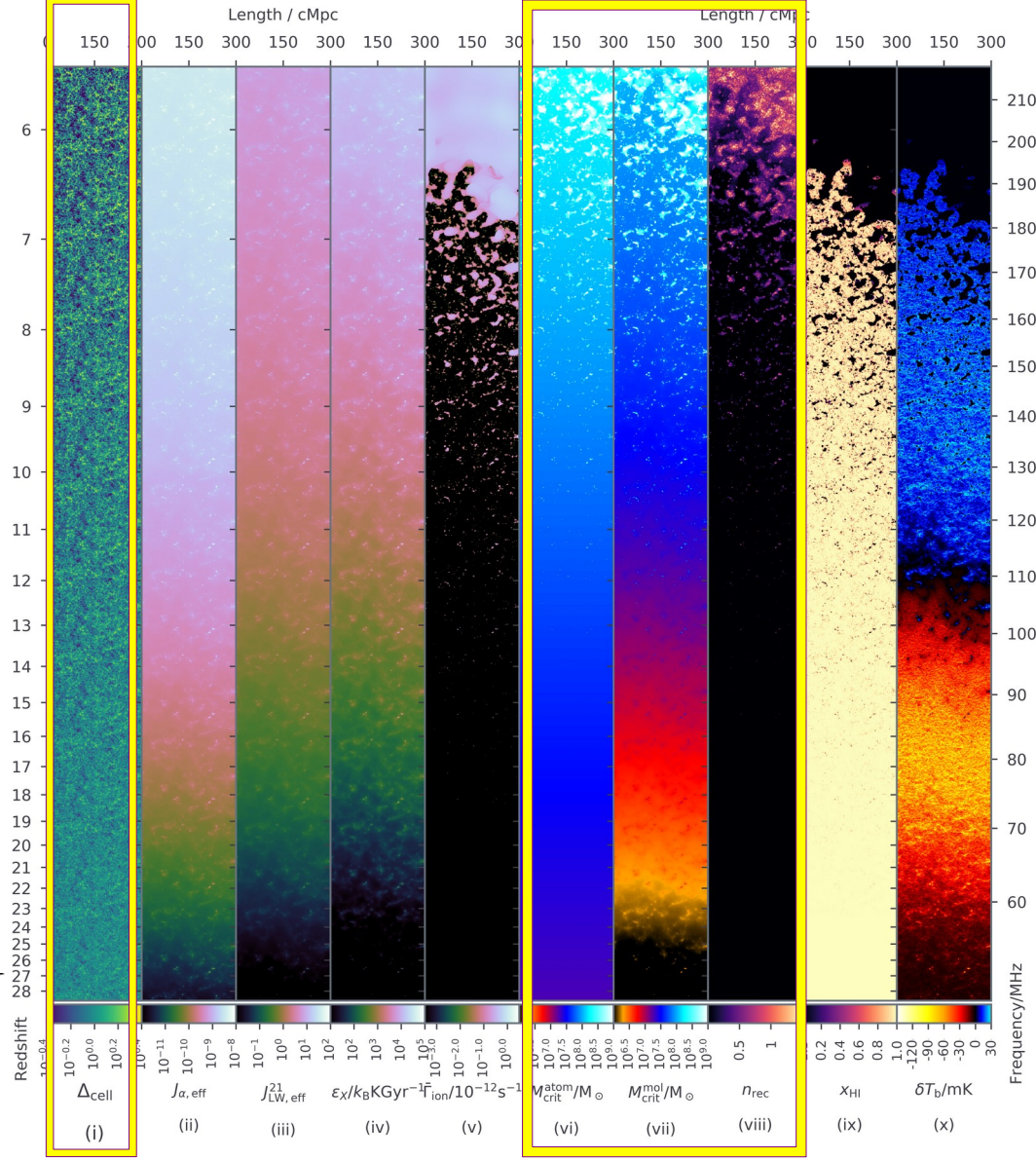
$$T_S^{-1} = \frac{T_{\text{CMB}}^{-1} + x_\alpha T_\alpha^{-1} + x_c T_K^{-1}}{1 + x_\alpha + x_c}$$

$x_\alpha \propto J_\alpha(z)$

Wouthuysen-Field effect (Ly α pumping)

$$x_c = x_c^{\text{HH}} + x_c^{\text{eH}} + x_c^{\text{pH}}$$

Collision coupling



Mesinger+ (2016)

$\delta(\mathbf{r}, z)$: Dark matter density fluctuations depends on structure formation

$x_{\text{HI}}(z)$: Volume neutral fraction depends on SFH in the early Universe

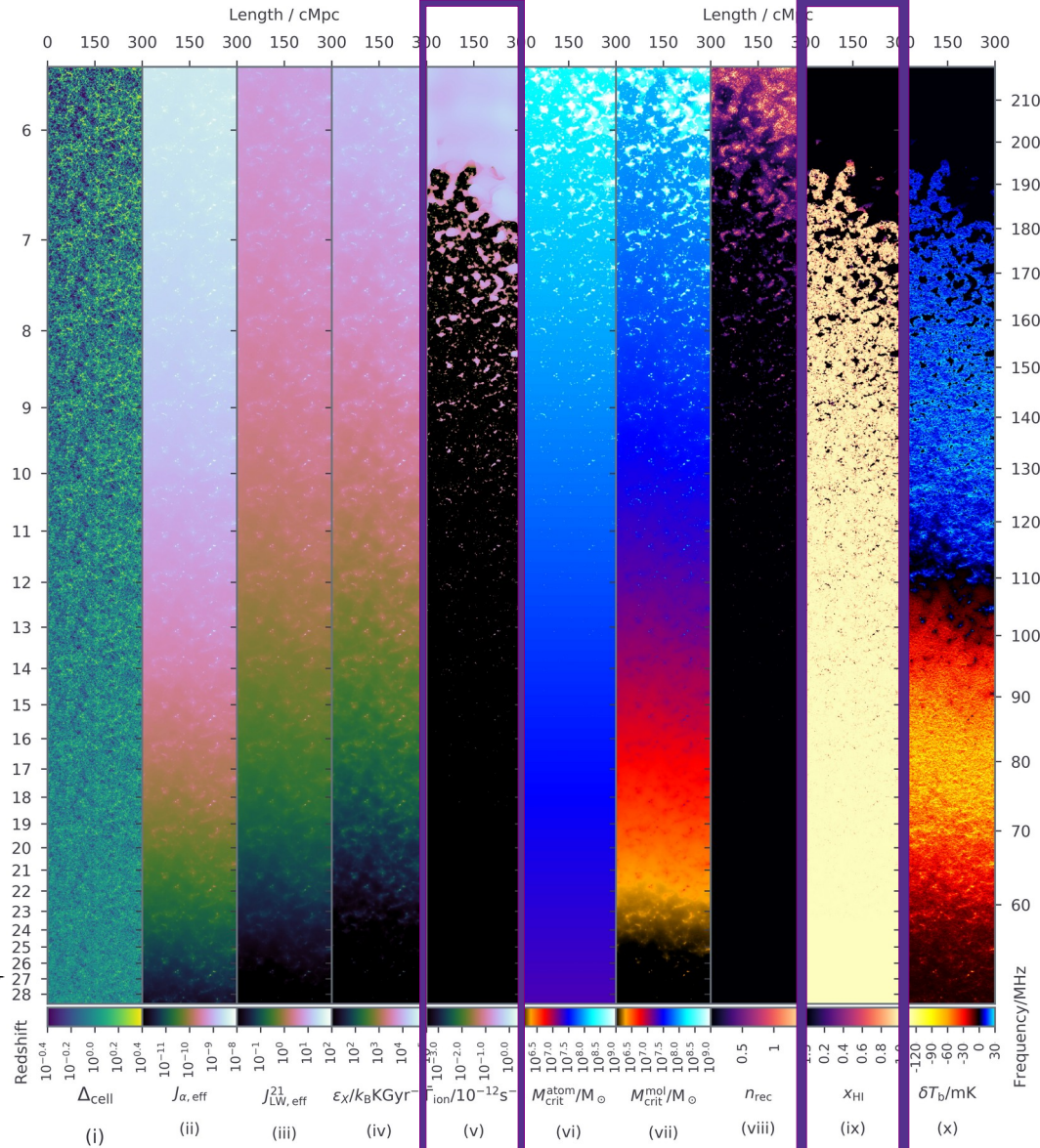
$$T_S^{-1} = \frac{T_{\text{CMB}}^{-1} + x_\alpha T_\alpha^{-1} + x_c T_K^{-1}}{1 + x_\alpha + x_c}$$

$x_\alpha \propto J_\alpha(z)$

Wouthuysen-Field effect (Ly α pumping)

$x_c = x_c^{\text{HH}} + x_c^{\text{eH}} + x_c^{\text{pH}}$

Collision coupling



Mesinger+ (2016)

$\delta(\mathbf{r}, z)$: Dark matter density fluctuations depends on structure formation

$x_{\text{HI}}(z)$: Volume neutral fraction depends on SFH in the early Universe

$$T_S^{-1} = \frac{T_{\text{CMB}}^{-1} + x_\alpha T_\alpha^{-1} + x_c T_K^{-1}}{1 + x_\alpha + x_c}$$

$x_\alpha \propto J_\alpha(z)$

Wouthuysen-Field effect (Ly α pumping)

$$x_c = x_c^{\text{HH}} + x_c^{\text{eH}} + x_c^{\text{pH}}$$

Collision coupling

